Food Analytical Methods (2026) 19:190
https://doi.org/10.1007/s12161-026-03089-6

RESEARCH

Analytical Profiling of Phenolic and Flavonoid Constituents in *Ononis angustissima* Using LC–ESI–MS/MS Coupled with Multivariate Optimization

Larbi Derbak[1] · Abdesselem Si Mohammed[2] · Mohamed Lamine Rabhi[3] · Hamdi Bendif[4] · Radia Ayad[5] · Khellaf Rebbas[6] · Ibrahim Demirtas[7] · Anis Ahmad Chaudhary[4] · Walid Elfalleh[4] · Stefania Garzoli[8]

Received: 6 January 2026 / Accepted: 26 March 2026 / Published online: 14 April 2026
© The Author(s) 2026, modified publication 2026

Abstract

Ononis angustissima, a member of the *Fabaceae* family long employed in folk remedies, has remained largely unexplored in terms of its phytochemical composition and bioactivity. In this work, we applied a face-centered central composite design to refine the ethanolic extraction process for phenolic and flavonoid constituents, achieving peak yields of 76.44 ± 0.76 mg GAE/g dry weight (dw) and 66.42 ± 0.83 mg QE/g dw, respectively. Comprehensive LC–ESI–MS/MS analysis unveiled nineteen principal metabolites, among which luteolin (143.55 ± 1.76 µg/g), salicylic acid (45.82 ± 0.24 µg/g dw), and trans-ferulic acid (40.53 ± 0.43 µg/g dw) were most abundant. The chloroform partition demonstrated remarkable butyrylcholinesterase inhibitory activity (IC_{50} of 20.52 ± 0.58 µg/mL), showing stronger activity than galantamine under the tested conditions. Additionally, the ethanolic extract exhibited pronounced, selective, and dose-dependent antiproliferative effects against the DLD-1 and CAPAN-1 tumor cell lines, with IC_{50} of 0.82 ± 0.07 and 0.87 ± 0.06 mg/mL, respectively, while showing considerably lower cytotoxicity toward the L929 fibroblasts. Molecular docking studies further predicted strong interactions of flavonoids, particularly luteolin and quercetin, with both acetylcholinesterase and butyrylcholinesterase active sites, underscoring their neuroprotective potential. Moreover, ADME profiling of the identified metabolites indicated generally favorable pharmacokinetic properties, with luteolin, caffeic acid, and trans-ferulic acid emerging as promising lead compounds due to their absorption potential, lipophilicity, and bioavailability. Collectively, these results highlight *O. angustissima* as a valuable source of bioactive compounds worthy of further investigation for potential anticancer and neuroprotective applications. However, given the in vitro and in silico nature of this study, additional research, including bioassay-guided isolation, mechanistic studies, and in vivo validation, is necessary to confirm its therapeutic relevance.

Keywords *Ononis angustissima* · Phenolic compounds · Flavonoids · LC–ESI–MS/MS · Antiproliferative activity · In silico analysis

✉ Hamdi Bendif
hlbendif@imamu.edu.sa

✉ Stefania Garzoli
stefania.garzoli@uniroma1.it

[1] Centre de Recherche en Technologies Agro-Alimentaires, Route de Targa Ouzemmour, Campus Universitaire, 06000 Bejaia, Algeria

[2] Laboratory of Environment and Sustainable Development, Department of Biological Sciences, Faculty of Nature and Life Sciences, Ahmed Zabana University of Relizane, 48000 Relizane, Algeria

[3] Saharan Area Laboratory for Agricultural Modernization and Advancement (SALAMA-LAB), Higher School of Saharan Agriculture, El-Oued, PB 90, El Oued 39011, Algeria

[4] Department of Biology, College of Science, Imam Mohammad Ibn Saud Islamic University (IMSIU), Riyadh 11623, Saudi Arabia

[5] Laboratory of Phytochemistry and Pharmacology, Department of Chemistry, Faculty of Exact Sciences and Informatics, University of Jijel, Jijel 18000, Algeria

[6] Department of Natural and Life Sciences, Faculty of Sciences, University of M'sila, University Pole, Road Bordj Bou Arreiridj, M'sila 28000, Algeria

[7] Department of Pharmaceutical Chemistry, Faculty of Pharmacy, Ondokuz Mayıs University, Samsun, Turkey

[8] Department of Chemistry and Technologies of Drug, Sapienza University, 00185 Rome, Italy

Introduction

Ononis angustissima Lam. (*O. angustissima*), a perennial subshrub of the Fabaceae family, is a lesser-known medicinal and aromatic plant endemic to North Africa and the Canary Islands, with notable distribution in semi-arid regions of Algeria, including Ouargla, Ghardaïa, Biskra, and Béchar (Al-Khalil et al. 1995; Merzag et al. 2017; POWO 2025). The genus *Ononis*, characterized by trifoliate leaves and papilionaceous flowers, is widely distributed in the Mediterranean basin and has been historically valued in traditional medicine for its diuretic, anti-inflammatory, and antidiabetic properties (Altuner et al. 2010; Al-Aboudi and Afifi 2011). *O. angustissima* is distinguished morphologically by its narrow, almost linear leaflets, spiny stems, and bright yellow flowers arranged in aerial clusters. Traditional use of *Ononis* species dates back centuries, with various parts of the plant, particularly roots and aerial organs, being employed in folk remedies for their diuretic, anti-inflammatory, and antidiabetic properties (Besbas 2020). Phytochemical studies on closely related *Ononis* species have revealed a rich profile of secondary metabolites, including flavonoids, phenolic acids, triterpenes, and essential oils, which are associated with their therapeutic activities (Altuner et al. 2010; Besbas 2020). In recent years, underutilized leguminous plants have attracted growing scientific interest as reservoirs of novel natural compounds with anti-proliferative and anti-enzymatic therapeutic potential (He et al. 2024; Eswaran et al. 2025). *O. angustissima* represents a promising candidate for the discovery of novel bioactive compounds, given its unique phytochemical background and traditional uses (Bouheroum et al. 2009; Ghribi et al. 2015; Benmeddour et al. 2024). However, despite this promising potential, *O. angustissima* remains largely unexplored both phytochemically and pharmacologically.

This work offers an in-depth examination of *O. angustissima's* aerial sections via a series of extractions using solvents of increasing polarity. Total phenolic and flavonoid concentrations were quantified, and liquid chromatography coupled with electrospray ionization tandem mass spectrometry (LC–ESI–MS/MS) was employed to elucidate the phenolic composition of the richest extract. Concurrently, enzyme inhibition and cytotoxic effects on both tumorigenic and healthy cell lines were evaluated. Lastly, key active constituents underwent computational ADME analysis and molecular docking to predict their pharmacokinetic behavior.

Material and Methods

Plant Material

The aerial parts of *O. angustissima* were collected in May 2023 from the M'sila region in northern Algeria. A reference specimen (No. KR0013) was taxonomically identified by Prof. K. Rebbas of the University of M'sila (Algeria) and is stored in his personal herbarium. The plant samples were rinsed with distilled water, air-dried at 25 °C in a dark, ventilated environment, and then ground into a fine powder. The powdered samples were subsequently stored at 4 °C for future analysis.

Table 1 The experimental response surface methodology parameters

Factors	Levels		
	− 1	0	1
X_1 (h)	24	48	72
X_2 (%)	50	70	90
X_3 (mL/g)	10	20	30

X_1 extraction time (h), X_2 solvent concentration (%), X_3 solid–liquid ratio obtained (mL/g)

TCP and TFC Optimized Extraction and Fractionation

The extraction of total phenolic content (TPC) and total flavonoid content (TFC) from the aerial parts of *O. angustissima* was performed using the maceration method. Ethanol–water mixtures were employed as the extraction solvents, and the process was conducted at 25 °C. A face-centered central composite design was applied according to the Kouteu et al. (2024) method, with slight modifications, to optimize the extraction procedure by assessing the influence of three independent variables: extraction duration (X_1), ethanol concentration (X_2), and solvent-to-solid ratio (X_3). These variables were modeled to determine their effect on the yield of TPC and TFC, with the optimal conditions established according to Table 1. Under optimized conditions (X_1: extraction time in hours; X_2: solvent concentration in percentage; X_3: solid–liquid ratio obtained in mL/g), 50 g of powdered plant material was macerated and filtered. The obtained extract was then concentrated under reduced pressure at 45 °C with a Büchi Rotavapor R-215 (Büchi Labortechnik AG, Switzerland). The resulting dry material was then dissolved in 100 mL of distilled water, heated to 100 °C, and sequentially partitioned against solvents of increasing polarity: chloroform, ethyl acetate, and *n*-butanol. For each partitioning step, 100 mL of the chosen solvent was combined with the hot aqueous solution and kept at room temperature to facilitate compound migration between phases. Each fractionation was performed twice to ensure reproducibility, and the organic layers were recovered and concentrated under reduced pressure at 45 °C.

TCP and TFC Quantification

Total phenolic content in the *O. angustissima* samples was assessed by the Folin–Ciocalteu assay (Müller et al. 2010).

Briefly, 20 µL of each extract (1 mg/mL) was pipetted into a 96-well plate, followed by 100 µL of Folin–Ciocalteu reagent (pre-diluted 1:9 v/v) and 75 µL of 7.5% Na_2CO_3. Plates were kept in the dark for 2 h before measuring absorbance at 765 nm. Quantification was achieved via a gallic acid calibration curve. Flavonoid levels were determined using the aluminum chloride colorimetric method (Topçu et al. 2006). To 50 µL of sample (1 mg/mL), 130 µL methanol, 10 µL of 10% $Al(NO_3)_3$, and 10 µL of 1 M potassium acetate were added. After a 45-min incubation at room temperature, absorbance was recorded at 415 nm, and concentrations were derived from a quercetin standard curve. All measurements were carried out in triplicate to ensure accuracy and reproducibility. Results are expressed as mean ± standard deviation (SD) of three independent experiments, with each experiment comprising three technical replicates.

LC–ESI–MS/MS Analysis and Settings

The ethanolic extract of *O. angustissima* was analysed by LC–ESI–MS/MS following the procedure of Derbak et al. (2025). Briefly, 50 mg of extract was dissolved in 1 mL each of methanol and *n*-hexane in a 2-mL Eppendorf tube, vortexed for 2 min at 4 °C (Bioprep-24 homogenizer), and centrifuged at 15,033 × *g* for 10 min using the centrifuge Hettich Universal 320 R. The methanol layer was collected, prepared at a 1:9 ratio with distilled water, and filtered through a Captiva premium nylon syringe filter (25 mm, 0.45 µm) before injection (5.12 µL). Chromatographic separation was performed on an Agilent 1260 Infinity II LC system coupled to an Agilent 6460 Triple Quadrupole Mass Spectrometer (ESI source), using a Poroshell 120 EC-C18 column (100 mm × 3.0 mm, 2.7 µm) maintained at 25 °C. The mobile phase consisted of acetonitrile (0.1% formic acid (B)) and water (5 mM ammonium formate (A)), held isocratically at a 75:25 ratio with solvent B, flowing at 0.5 mL/min over a 30-min run. Data acquisition was carried out in both positive and negative ion modes (ESI + and ESI −) with multiple reaction monitoring (MRM) using Agilent Mass Hunter software. Optimized collision energy parameters were applied to improve ion fragmentation and transmission. The MS conditions included a capillary voltage of 4000 V, with the drying gas heated to 350 °C and nitrogen delivered at 11 mL/min for nebulization and 15 mL/min for desolvation (Rabhi et al. 2025). Method validation was performed following the approach described by Yilmaz (2020) to evaluate analytical performance in terms of linearity and sensitivity. Quantification of phenolic compounds was carried out using external calibration curves prepared from authentic standards at several concentration levels covering the working range. Calibration curves were obtained by plotting peak area against analyte concentration using linear regression, and linearity was assessed through the correlation coefficient (R^2). Sensitivity of the method was evaluated by determining the limits of detection (LOD) and limits of quantification (LOQ) based on signal-to-noise ratios of 3 and 10, respectively.

In Vitro Anti-enzymatic Activity Evaluation

The inhibitory activities against acetylcholinesterase (AChE) and butyrylcholinesterase (BChE) were evaluated following Ellman's method (Ellman et al. 1961) with slight modifications. Ten microliters of ethanolic extract of *O. angustissima* was mixed with 150 µL of sodium phosphate buffer (100 mM, pH 8.0), followed by 20 µL of AChE (5.32×10^{-3} U) or BChE (6.85×10^{-3} U). After incubation for 15 min at 25 °C, 10 µL of DTNB (0.5 mM) and 10 µL of acetylthiocholine iodide (0.71 mM) or butyrylthiocholine chloride (0.2 mM) were added. Absorbance was measured at 412 nm at 0-, 5-, 10-, and 15 min. Inhibition percentage (I %) was determined using the following formula:

$$I(\%) = \frac{A_c - A_e}{A_c}$$

where A_c and A_e represent the absorbance of control and extract-treated samples, respectively. Galantamine hydrobromide was used as a positive control. All assays were performed in triplicate for each extract concentration. Results are expressed as mean IC_{50} values (µg/mL) ± SD calculated from three independent experiments.

In Vitro Anti-proliferative Activity Evaluation

The cytotoxic effects of *O. angustissima* ethanolic extract were examined against two human cancer cell lines, pancreatic carcinoma (CAPAN-1) and colorectal adenocarcinoma (DLD-1), as well as a non-tumorigenic fibroblast line (L929). All cell lines were provided by the laboratory of Prof. Dr. Mustafa Türk (Kırıkkale University, Türkiye). Cells were cultured in Corning (USA) 96-well plates using complete Sigma-Aldrich's Dulbecco's modified Eagle's medium (DMEM) enriched with the necessary growth supplements. The antiproliferative activity was evaluated via the MTT colorimetric assay following protocols documented by Boncler et al. (2013) with minor adaptations. Briefly, 10,000 cells were seeded into each individual well and incubated for 24 h, then treated with gradient doses of the *O. angustissima* ethanolic extract (0.25, 0.5, 0.75, and 1 mg/mL) dissolved in complete culture medium. After another 24 h, the treatment medium was removed and replaced with 100 µL of MTT reagent (1 mg/mL in PBS; Sigma-Aldrich, USA). Plates were incubated in the dark at 37 °C for 2 h to permit formazan formation. Subsequently, the supernatant was discarded, and formazan crystals were solubilized in 100 µL isopropanol

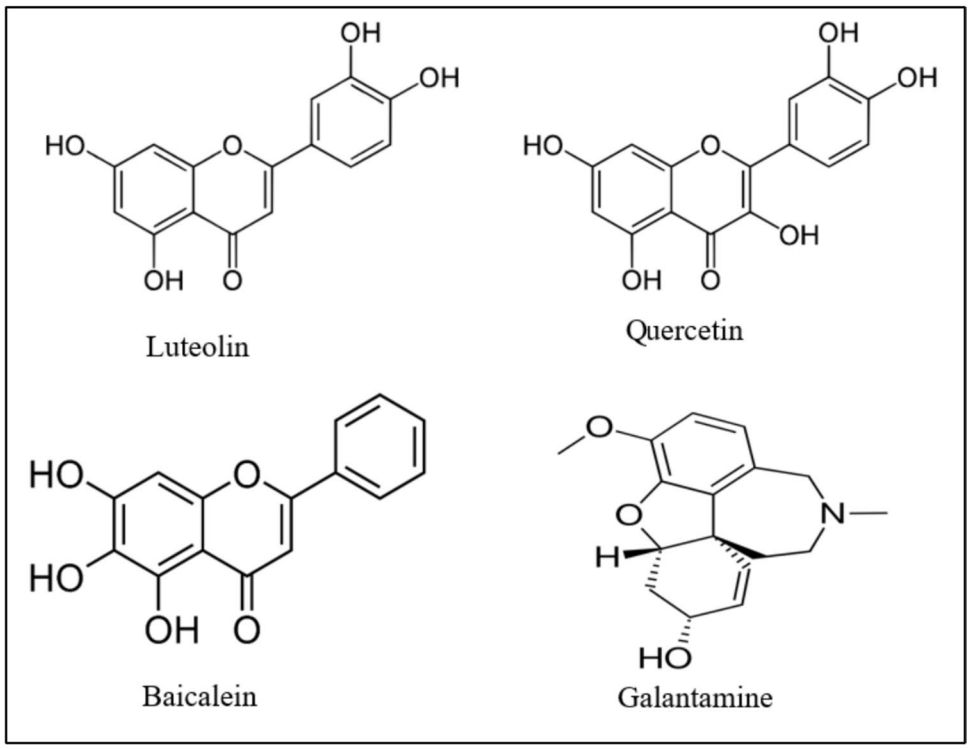


Fig. 1 Structures of ligand molecules used for molecular docking

(Merck, Germany). Absorbance was then read at 570 nm on a Thermo Scientific Multiskan GO microplate reader. Cell viability was expressed as a percentage relative to untreated controls, calculated using the equation:

$$\text{Cells viability percentage } (\%) = 100 - \left(\frac{A_s}{A_c}\right) \times 100$$

where A_s represents the absorbance of treated cells and A_c represents the absorbance of control cells. All assays were performed in triplicate for each extract concentration. Results are expressed as mean IC_{50} values (µg/mL) ± SD calculated from three independent experiments.

In Silico Analysis

ADME

The bioavailability of the identified phytochemicals was estimated using in silico predictive approaches based on key physicochemical parameters, including molecular weight, lipophilicity, polarity, and aqueous solubility, as described by Mhadhbi et al. (2023). In addition, their pharmacokinetic profiles were evaluated through ADME (absorption, distribution, metabolism, and excretion) modeling to explore their potential as drug-like candidates (Derbak et al. 2024). These computational predictions provide preliminary insights into the pharmacokinetic behavior of the compounds and should be considered as hypothesis-generating tools that require further experimental validation.

Molecular Docking

Molecular docking analyses were conducted to evaluate the interactions of four selected ligand (Fig. 1): luteolin (2-(3,4-dihydroxyphenyl)−5,7-dihydroxy-4H-chromen-4-one; $C_{15}H_{10}O_6$, PubChem CID: 5,280,445), quercetin (2-(3,4-dihydroxyphenyl)−3,5,7-trihydroxy-4H-chromen-4-one; $C_{15}H_{10}O_7$, PubChem CID: 5,280,343), baicalein (5,6,7-trihydroxy-2-phenyl-4H-chromen-4-one; $C_{15}H_{10}O_5$, PubChem CID: 5,281,605), and galantamine ((4aS,6R,8aS)−4a,5,9,10,11,12-hexahydro-3-methoxy-11-methyl-6H-benzofuro[3a,3,2-ef][2]benzazepin-6-ol; $C_{17}H_{21}NO_3$, PubChem CID: 9651) with two Alzheimer's disease-related enzymes: AChE and BChE. The crystal structures of human AChE (PDB ID: 4PQE) and BChE (PDB ID: 4BDS) were retrieved from the Protein Data Bank (www.rcsb.org). Prior to docking, all crystallographic water molecules were removed, and polar hydrogens, as well as Kollman charges, were added using AutoDockTools (ADT) version 1.5.7. Ligands were energy-minimized, converted to pdbqt format, and prepared for flexible docking. Docking simulations were performed using AutoDock Vina, and the binding affinities (kcal/mol) of each ligand were calculated. The best-scoring conformations were selected based on docking energy and key interactions, such as hydrogen

Table 2 Factorial design and response measurements in the optimization of *Ononis angustissima* extraction

Test	X_1 (h)	X_2 (%)	X_3 (mL/g)	TPC (mg GAE/g dw)	TFC (mg QE/g dw)
1	72	90	30	71,53 ± 0.34	66.42 ± 0.79
2	72	90	10	36.51 ± 0.41	39.11 ± 0.14
3	72	70	20	56.5 ± 0.24	44.46 ± 0.27
4	72	50	30	35.92 ± 0.12	23.26 ± 0.10
5	72	50	10	45.84 ± 0.39	27.52 ± 0.11
6	48	90	20	47.0 ± 0.21	44.76 ± 0.32
7	48	70	20	65.0 ± 0.41	41.2 ± 0.19
8	48	70	20	64.85 ± 0.23	42.06 ± 0.25
9	48	70	20	64.8 ± 0.45	42.0 ± 0.17
10	48	70	20	64.9 ± 0.67	42.0 ± 0.19
11	48	70	20	65.8 ± 0.49	41.6 ± 0.31
12	48	70	20	65.87 ± 0.41	43.0 ± 0.12
13	48	70	10	37.83 ± 0.30	28.75 ± 0.13
14	48	70	30	76.44 ± 0.64	55.8 ± 0.31
15	48	50	20	66.24 ± 0.27	49.0 ± 0.25
16	24	90	30	65.02 ± 0.39	55.43 ± 0.30
17	24	90	10	34.88 ± 0.15	27.92 ± 0.12
18	24	70	20	52.38 ± 0.32	36.36 ± 0.21
19	24	50	30	18.94 ± 0.22	8.95 ± 0.11
20	24	50	10	41.2 ± 0.33	26.88 ± 0.26
R^2				80.3%	81.8%
Adjusted R^2				75.2%	76.4%
Predicted R^2				71.5%	72.8%

Values are presented as means ± standard deviation (SD) from three independent replicates

X_1 extraction time, X_2 solvent concentration, X_3 liquid/solid ratio, *TPC* total phenolic content, *TFC* total flavonoid content, *GAE* gallic acid equivalents, *dw* dry weight, *QE* quercetin equivalent, R^2 coefficient of determination

bonds, π–π stacking, and hydrophobic contacts, which were further analyzed using Discovery Studio Visualizer.

Statistical Analysis

All statistical analyses were conducted using Minitab 19 (Minitab Inc., USA), with response surface plots generated in Statistica 10 (StatSoft, France). Data are presented as mean ± standard deviation of three independent experiments ($n = 3$), with each experiment comprising three technical replicates for TPC, TFC, enzyme inhibition, and cytotoxicity assays. Model adequacy was verified through ANOVA, lack-of-fit testing, and the coefficient of determination (R^2). Tukey's multiple range test was applied for post hoc comparisons, with statistical significance set at $p < 0.05$. For IC_{50} calculations, non-linear regression analysis was performed using GraphPad Prism (version 9.0), with values expressed as mean ± SD from three independent experiments.

Results and Discussion

Extraction Optimization

The maceration extraction of TPC and TFC from *O. angustissima* aerial parts was optimized by evaluating the effects of extraction time, solvent concentration, and liquid-to-solid ratio. The face-centered central composite design within a response surface methodology framework was employed to assess and model the extraction efficiency. The results of the 20 experimental tests are presented in Table 2.

The powdered extracts of *O. angustissima* demonstrated considerable variation in their total phenolic and flavonoid contents. Total phenolic concentrations ranged from 18.94 ± 0.22 to 76.44 ± 0.64 mg GAE/g dry weight (dw), whereas total flavonoid levels varied between 8.95 ± 0.11 and 66.42 ± 0.79 mg QE/g dw. A regression analysis was carried out on the experimental dataset to assess the statistical relevance of model coefficients influencing the extraction yield of phenolic and flavonoid constituents. As presented in Table 2, the coefficients of determination values were 0.803 for TPC and 0.818 for TFC, indicating a significant

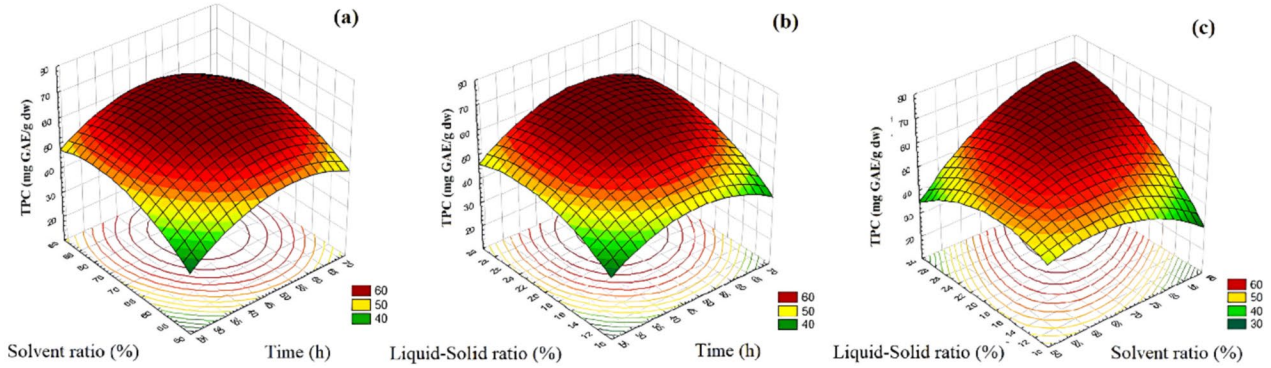


Fig. 2 Response surface plots indicating combined effects of maceration parameters on TPC: **a** time and solvent ratio, **b** time and liquid–solid ratio, and (**c**) solvent ratio and liquid–solid ratio

correlation between the predictive model and the observed experimental outcomes. The relationships between solvent percentage, extraction time, and liquid-to-solid ratio and their impact on phenolic and flavonoid yields are mathematically described in Eqs. 1 and 2, respectively.

$$\begin{aligned} \mathrm{TPC} = {} & -27.596 + 1.649X_1 + 1.424X_2 - 1.621X_3 \\ & - 0.015{X_1}^2 - 0.016{X_2}^2 - 0.058{X_3}^2 - 0.004X_1X_2 \\ & + 0.009X_1X_3 + 0.061X_2X_3 \end{aligned} \quad (1)$$

$$\begin{aligned} \mathrm{TFC} = {} & 41.455 + 0.855X_1 - 0.857X_2 - 1.603X_3 \\ & - 0.01{X_1}^2 + 0.002{X_2}^2 - 0.038{X_3}^2 \\ & + 0.002X_1X_2 + 0.007X_1X_3 + 0.048X_2X_3 \end{aligned} \quad (2)$$

The results obtained from multiple regression analysis were consistent with those derived from response surface analysis for both TPC and TFC, as illustrated in Figs. 2 and 3. The influence of extraction time and ethanol concentration on polyphenol yield is depicted in Fig. 2a, whereas their effects on flavonoid content are presented in Fig. 3a.

Among the studied factors, extraction time proved to be a dominant factor, exhibiting a strong quadratic influence in addition to its positive linear trend. The most elevated TPC readings occurred within the 65–75% ethanol concentration range and extraction durations between 45 and 55 h. In parallel, maximum flavonoid concentrations were achieved within an ethanol concentration range of 80% to 90% and an extraction time window of 50 to 65 h. These findings align with previous reports highlighting that the use of aqueous-organic solvent mixtures creates a moderately polar extraction medium, thereby enhancing solvent-matrix interactions (Paniwnyk et al. 2009). Figure 2b depicts the combined impacts of extraction duration and liquid-to-solid ratio on polyphenol concentration, while Fig. 3b illustrates these parameters' impact on flavonoid yield. The extraction of polyphenols peaked at 60 h with a liquid-to-solid ratio of less than 1 g/24 mL. Maximum flavonoid yield was similarly observed at 60 h with a corresponding ratio below 1 g/20 mL. These results confirm that plant material concentration exerts a significant influence on the extraction efficiency of both compound

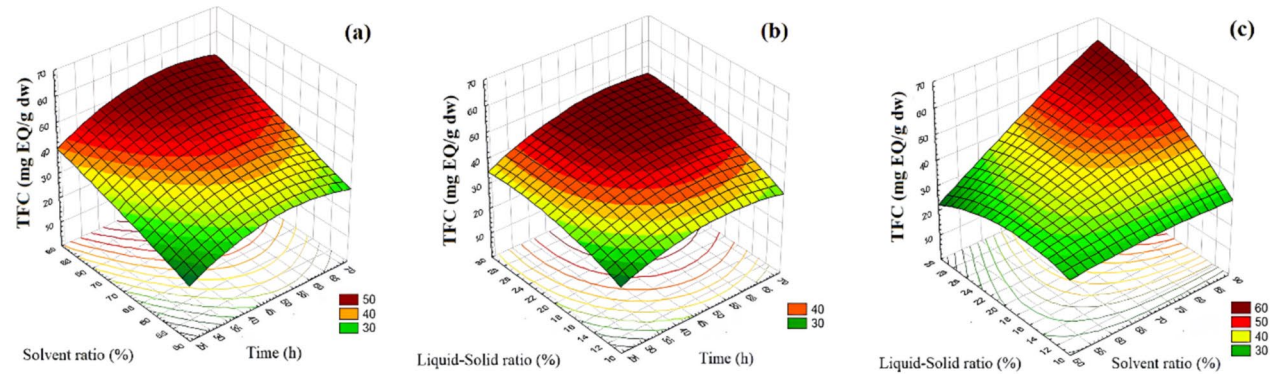


Fig. 3 Response surface plots indicating combined effects of maceration parameters on TFC: **a** time and solvent ratio, **b** time and liquid–solid ratio, and (**c**) solvent ratio and liquid–solid ratio

classes (Zhang et al. 2018). Furthermore, the influence of ethanol-to-water ratio and liquid-to-solid ratio on the recovery of phenolics and flavonoids was notably evident, as demonstrated in Fig. 2c for polyphenols, and Fig. 3c for flavonoids. Polyphenol extraction was optimized at ethanol concentrations exceeding 85%, whereas optimal flavonoid recovery was achieved at ethanol levels above 85% as well (Fig. 4). These trends underscore the solvent system's critical role in modulating the extractability of bioactive compounds across different plant matrices (Mungwari et al. 2024).

The R^2 values (80.3% for TPC, 81.8% for TFC) confirm that the response surface models adequately capture the relationship between extraction parameters and yields, aligning with reported ranges for medicinal plant optimization, where $R^2 > 75\%$ is considered satisfactory due to inherent material variability (Nissar et al. 2024). The adjusted R^2 values (75.2% for TPC, 76.4% for TFC) were close to their respective R^2 values, indicating that non-significant terms did not cause model overfitting. Additionally, the predicted R^2 values (71.5% for TPC, 72.8% for TFC) showed reasonable agreement with adjusted R^2, further supporting the models' predictive capability.

Table 3 Estimated optimal conditions and predicted and experimental values of the investigated responses

Optimum extraction parameters		
X_1 (h)	X_2 (%)	X_3 (mL/g)
72	90.00	30
Response variables TPC (mg GAE/g dw)		
Predicted	Experimental	
71.25	76.44 ± 0.76	
Response variables TPC (mg QE/g dw)		
Predicted	Experimental	
67.55	66.42 ± 0.83	

Values are presented as means ± standard deviation (SD) from three independent replicates

X_1 extraction time, X_2 solvent concentration, X_3 liquid/solid ratio, *GAE* gallic acid equivalents, *dw* dry weight, *QE* quercetin equivalent

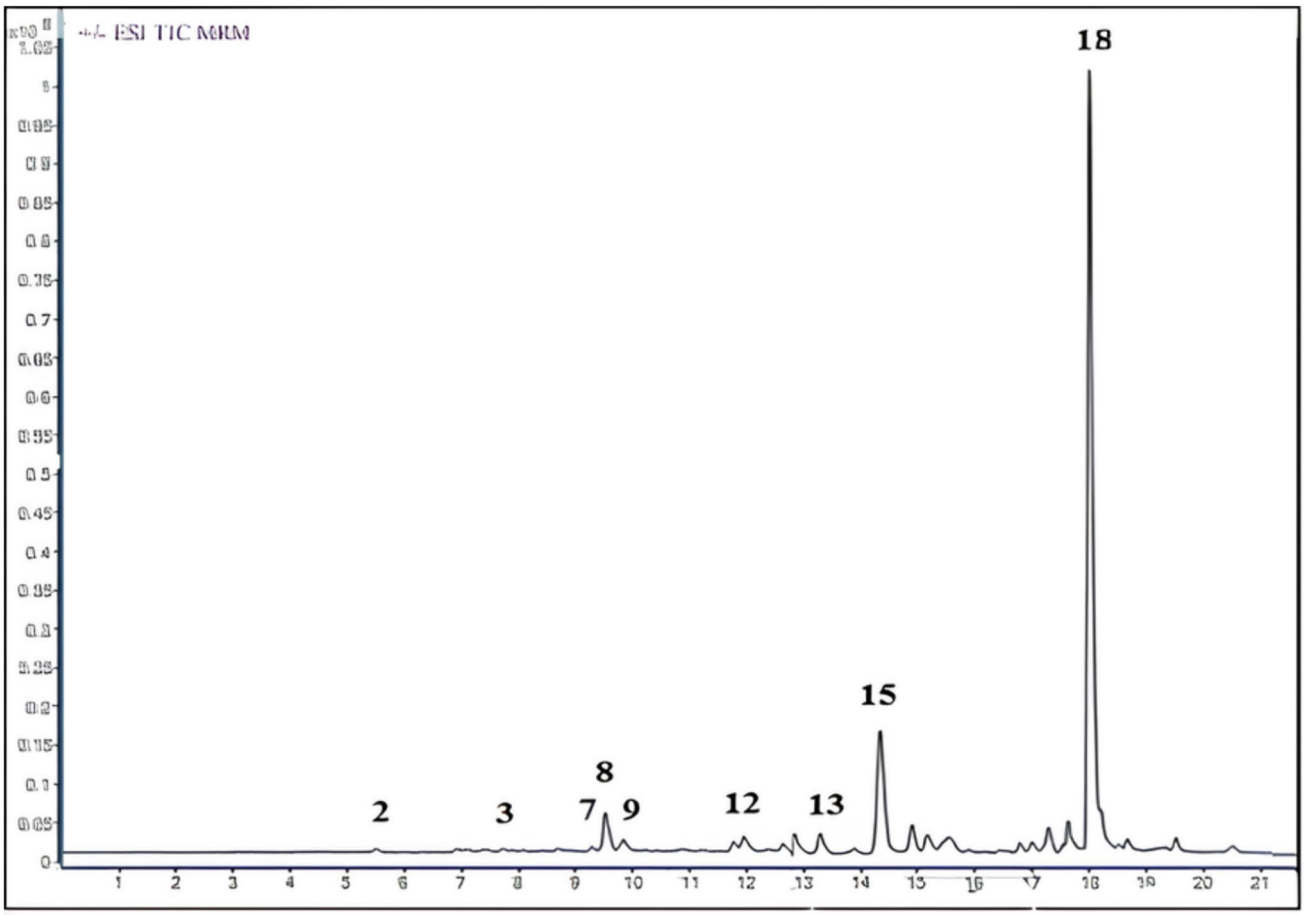


Fig. 4 LC–ESI–MS/MS-based chemical profiling of the ethanolic extract of *Ononis angustissima*. 1, gallic acid; 2, protocatechuic acid; 3, chlorogenic acid; 4, hydroxybenzaldehyde; 5, caffeic acid; 6. vanillin; 7, o-coumaric acid; 8, salicylic acid; 9, taxifolin; 10, trans-ferulic acid; 11, hesperidin; 12, isoquercitrin; 13, kaempferol-3-glucoside; 14, chrysin; 15, trans-cinnamic acid; 16, quercetin; 17, baicalein; 18, luteolin; 19, biochanin A

Based on these results, the optimal extraction conditions and predicted response values were determined using a desirability function approach, with desirability scores ranging from 0.95 to 1.0, where 1.0 indicates the most desirable outcome. To experimentally validate the model, three independent replicate extractions were performed using the optimal parameters identified through response surface methodology (extraction time: 72 h, ethanol concentration: 90%, liquid-to-solid ratio: 30 mL/g). The validation results are summarized in Table 3.

LC–ESI–MS/MS Analysis

To further elucidate the chemical composition of the ethanolic extract of *O. angustissima*, this study employed liquid chromatography coupled with electrospray ionization mass spectrometry (LC–ESI–MS), a highly effective analytical technique (Benouchenne et al. 2020). LC–MS methods are widely recognized for their ability to significantly advance phytochemical investigations due to the biochemical diversity of plant matrices. These techniques enable efficient separation and detection of a broad range of semi-polar compounds, including major classes of secondary metabolites (El Sayed et al. 2020). The ethanolic extract was selected for LC–ESI–MS/MS profiling as it constitutes the parent extract from which all fractions were obtained via liquid–liquid partitioning. This strategy ensures a comprehensive phytochemical characterization of *O. angustissima* and provides a chemical foundation for the subsequent identification of bioactive constituents in any active fraction. The chemical composition of the ethanolic extract of *O. angustissima*, determined by LC–ESI–MS/MS analysis, is presented in Table 4.

According to Table 4, a total of 19 compounds were identified and quantified in the ethanolic extract of *O. angustissima*. The most abundant compound was luteolin, which was present at a concentration of 143.55 ± 1.76 µg/g dw of extract, followed by salicylic acid at 45.82 ± 0.24 µg/g dw, trans-ferulic acid at 40.53 ± 0.43 µg/g dw, and o-coumaric acid at 26.56 ± 0.76 µg/g dw. Luteolin, a flavonoid commonly found in medicinal plants, is recognized for its significant anticancer properties (Ganai et al. 2021). It exerts its therapeutic effects by inhibiting tumor cell proliferation, protecting against carcinogenic agents, and inducing apoptosis through various molecular signaling pathways (Imran et al. 2019). Additionally, other bioactive compounds with substantial therapeutic potential were detected in the ethanolic extract of *O. angustissima*. Similarly, salicylic acid, although primarily recognized for its keratolytic and anti-inflammatory roles, also exhibits anti-cancerous properties by promoting apoptosis through increased nitric oxide production (Ausina et al. 2020). Trans-ferulic acid, known for its potent antioxidant capacity and role in mitigating oxidative stress, was linked with improved cholinesterase inhibition and neuroprotective effects against Alzheimer's disease, further enhancing the functional value of the extract (Singh et al. 2020; Bhuia et al. 2024). Moderate levels of isoquercitrin, kaempferol-3-glucoside, and quercetin were detected, all of which are flavonoids with strong free radical scavenging activity and established pharmacological effects, including anti-cancer properties (Azeem et al. 2022; Karimi and Valizadeh 2023; Liu et al. 2023).

Taxifolin, known for its promising effects on tumor management, microbial infections, oxidative stress, and cardiovascular and hepatic disorders, also displays enhanced anticancer activity (Sunil and Xu 2019). Baicalein, another noteworthy compound, has demonstrated considerable therapeutic potential in the treatment of Alzheimer's and Parkinson's diseases. Its pharmacological activities include reducing oxidative stress, inhibiting amyloid protein aggregation, and promoting neurogenesis and neuronal differentiation (Li et al. 2017). The high concentration of phenolic compounds with notable therapeutic properties in the ethanolic extract of *O. angustissima* emphasizes the importance of further exploring their biological activities, including antioxidant activity, free radical scavenging, and the inhibition of cancer cell proliferation.

The findings of this investigation are consistent with prior phytochemical studies of the *Ononis* genus, which is well-documented for its high phenolic content and associated bioactivities (Mhamdi et al. 2015; Mezrag et al. 2017; Youssef et al. 2024). The presence of gallic acid, chlorogenic acid, caffeic acid, vanillin, and quercetin in the methanolic extract of *Ononis natrix*, with gallic acid identified as the predominant constituent, was reported by Youssef et al. (2024). Additionally, Stojković et al. (2020) identified caffeic acid, kaempferol-3-*O*-glucoside, and various quercetin derivatives in *Ononis spinosa*. The profiling of structurally and functionally related phenolic compounds in *O. angustissima* provides compelling chemotaxonomic evidence and underscores its value as a potent source of pharmacologically important metabolites.

Anti-Enzymatic Activity

The ethanol, chloroform, ethyl acetate, and n-butanol extracts of *O. angustissima* were assessed for their anti-enzymatic activity through enzyme inhibition assays targeting Alzheimer's disease-related enzymes (AChE and BChE). The inhibitory potential of these extracts, expressed as IC_{50} values, was compared with that of the reference standard, galantamine, and the results are presented in Table 5.

According to the anti-enzymatic activity results, the chloroform extract of *O. angustissima* was the only fraction to exhibit significant BChE inhibition, with an IC_{50} value of 20.52 ± 0.58 µg/mL. This observed activity stems from the complex phytochemical mixture present in the chloroform

Table 4 LC–ESI–MS/MS characterization of the ethanolic extract of *Ononis angustissima*

No	RT (min)	Compound	Concentration (µg/g of extract)	Ion source	Ion transitions	Ion mode	R^2	LOQ (µg/L)	LOD (µg/L)	Linearity range (µg/L)	Intra-day precision[a] (RSD %)	Inter-day precision[b] (RSD %)	Recovery[c] (%)
1	3.104	Gallic acid	6.67 ± 0.02	ESI	169.0 → 125.0	Negative	0.998	10.50	3.20	15.625–250	2.3	2.9	98.2 ± 2.1
2	5.897	Protocatechuic acid	8.34 ± 0.03	ESI	153.0 → 109.0	Negative	0.997	13.173	3.151	15.625–250	2.8	3.4	96.7 ± 2.8
3	7.584	Chlorogenic acid	7.38 ± 0.02	ESI	353.0 → 191.0	Negative	0.998	25.902	11.589	31.25–500	3.1	3.8	95.3 ± 3.2
4	7.9236	Hydroxybenzaldehyde	4.86 ± 0.03	ESI	121.0 → 92.0	Negative	0.999	12.865	4.9742	15.625–250	1.9	2.5	101.2 ± 1.9
5	8.0313	Caffeic acid	2.80 ± 0.01	ESI	178.9 → 135.1	Negative	0.999	24.34	6.9505	31.25–500	2.1	2.7	99.4 ± 2.2
6	8.716	Vanillin	5.10 ± 0.10	ESI	153.0 → 125.0	Positive	0.995	40.541	14.588	62.5–1000	3.9	4.6	94.1 ± 3.7
7	9.377	o-Coumaric acid	26.56 ± 0.76	ESI	163.0 → 119.1	Negative	0.999	7.578	4.0983	15.625–500	1.8	2.4	102.5 ± 1.7
8	9.753	Salicylic acid	45.82 ± 0.24	ESI	137.0 → 93.1	Negative	0.999	82.465	47.669	112.5–1800	4.6	5.2	92.3 ± 4.5
9	9.803	Taxifolin	3.17 ± 0.12	ESI	303.0 → 285.0	Negative	0.997	18.42	6.13	31.25–1000	3.2	3.9	95.8 ± 3.1
10	10.088	trans-ferulic acid	40.53 ± 0.43	ESI	193.1 → 133.9	Negative	0.995	11.5276	6.1184	31.25–1000	2.7	3.3	97.9 ± 2.6
11	11.616	Hesperidin	0.22 ± 0.00	ESI	611.0 → 302.9	Positive	0.996	17.687	4.1396	31.25–500	3.4	4.1	93.6 ± 3.4
12	11.656	Isoquercitrin	17.57 ± 0.12	ESI	464.9 → 302.8	Positive	0.998	11.268	9.9382	18.75–300	2.4	3.0	100.8 ± 2.3
13	13.198	Kaempferol-3-glucoside	13.81 ± 0.31	ESI	448.8 → 286.9	Positive	0.999	4.5238	1.1609	7.8125–125	2.0	2.6	103.4 ± 1.9
14	14.187	Chrysin	0.64 ± 0.11	ESI	253.0 → 143.0	Positive	0.997	21.35	7.11	31.25–500	3.5	4.2	94.8 ± 3.5
15	14.289	Trans-cinnamic acid	14.58 ± 0.21	ESI	147.0 → 103.0	Positive	0.999	22.132	11.185	31.25–500	2.6	3.2	98.7 ± 2.5
16	14.838	Quercetin	10.31 ± 0.11	ESI	300.8 → 151.0	Negative	0.996	16.834	4.6558	27.5–440	3.0	3.7	96.2 ± 3.0
17	17.067	Baicalein	0.86 ± 0.01	ESI	271.0 → 123.0	Positive	0.997	19.63	6.54	31.25–500	3.3	4.0	95.1 ± 3.3
18	17.943	Luteolin	143.55 ± 1.76	ESI	285.0 → 133.0	Negative	0.996	15.21	5.07	31.25–500	2.5	3.1	99.6 ± 2.4
19	17.926	Biochanin A	2.53 ± 0.02	ESI	285.0 → 270.0	Positive	0.998	17.88	5.96	31.25–500	2.9	3.5	97.3 ± 2.8

RT retention time, R^2 coefficient of determination, *LOQ*/*LOD* limit of quantification/detection

[a]Intra-day precision expressed as relative standard deviation (RSD%) from six replicate analyses within the same day at a medium concentration level

[b]Inter-day precision expressed as RSD% from analyses on three consecutive days (six replicates per day) at a medium concentration level

[c]Recovery (%) expressed as mean ± SD from spiking experiments at three concentration levels (low, medium, high) performed in triplicate

Table 5 In vitro Alzheimer's inhibitory activity of *Ononis angustissima* extracts

Extract	AChE IC_{50} (µg/mL)	BChE IC_{50} (µg/mL)
Ethanol	> 200	> 200
Chloroform	> 200	20.52 ± 0.58^{a}
Ethyl acetate	> 200	> 200
n-Butanol	> 200	> 200
Galantamine	6.27 ± 0.36	34.75 ± 1.99^{b}

Values within each column followed by different superscript letters (a or b) indicate significant differences ($p < 0.05$). Results are expressed as mean ± SD from three independent experiments

AChE acetylcholinesterase, *BChE* butyrylcholinesterase

fraction rather than a single isolated compound, with synergistic or additive interactions among multiple constituents likely contributing to the overall inhibitory effect (Vaou et al. 2022). Under the tested in vitro conditions, the chloroform fraction showed stronger inhibitory activity (lower IC_{50}) than galantamine (34.75 ± 1.99 µg/mL), a reference standard included for benchmarking purposes. This comparison reflects relative performance in the enzymatic assay and should not be construed as direct therapeutic equivalence. The stronger inhibition of BChE compared to AChE suggests that the bioactive compounds in *O. angustissima* may have a greater affinity for BChE's broader active site, which is known to accommodate a wider range of ligands due to its larger size and more open structure compared with AChE (Fang et al. 2011; Revadigar et al. 2014). BChE inhibition has attracted growing interest due to its therapeutic relevance in Alzheimer's disease (AD). AD is a progressive neurodegenerative disorder characterized by cognitive decline, memory impairment, and cholinergic deficits, which are linked to decreased acetylcholine (ACh) levels in the brain (Chen et al. 2022). Both AChE and BChE play key roles in regulating ACh levels: AChE dominates in the healthy brain and in early AD, while BChE activity progressively increases as AChE activity declines in later stages of the disease (Chen et al. 2017). Consequently, BChE inhibitors are particularly important for advanced AD management, complementing or offering more benefits than AChE inhibition (Zhou et al. 2019; Sadeghi et al. 2024).

While several synthetic cholinesterase inhibitors such as donepezil, rivastigmine, and galantamine are widely used for AD treatment, their clinical benefits remain limited due to side effects, short half-life, and tolerance issues (Gidaro et al. 2015). In this context, natural products and plant-derived compounds have emerged as a promising alternative due to their structural diversity, multitarget potential, and generally lower toxicity (Gökhan et al. 2015). Notably, many flavonoids and phenolic acids reported in *O. angustissima*, such as luteolin, quercetin, and baicalein, have been associated with dual antioxidant and cholinesterase inhibitory activities (Katalinić et al. 2009; Olennikov et al. 2017; Liao et al. 2022a, b). The high luteolin content (143.55 ± 1.76 µg/g dw) in our LC–MS/MS analysis suggests that this compound, along with other flavonoids, may be contributing significantly to the observed BChE inhibition, as luteolin has been previously identified as a potent and selective BChE inhibitor (Katalinić et al. 2009). In addition, cholinesterase inhibitors have been linked to potential benefits in metabolic disorders such as diabetes mellitus, where BChE activity is often elevated and associated with insulin resistance and metabolic dysregulation (Vujanović et al. 2019). Thus, the significant BChE inhibitory effect observed for the chloroform fraction of *O. angustissima* suggests potential interest for further investigation in the context of neurodegenerative and metabolic disorders.

Cytotoxicity of the *O. angustissima* Ethanolic Extract

To explore the biomedical relevance of *O. angustissima*, its ethanolic extract was tested for antiproliferative effects on three different cell lines: CAPAN-1, DLD-1, and L929. CAPAN-1 and DLD-1 cell lines were selected due to the well-established role of oxidative stress and chronic inflammation in the initiation and progression of pancreatic and colorectal cancers (Mouillet-Richard et al. 2021; Ameur et al. 2024). The L929 fibroblast cell line served as a non-malignant control to determine the selectivity and potential safety of the extract toward healthy cells (Alshabi et al. 2022). The concentration range tested (0.25–1 mg/mL) was determined from prior screening assays, which indicated negligible cytotoxic effects below 0.25 mg/mL, ensuring the relevance of the selected doses for observing biologically meaningful antiproliferative effects.

The extract exhibited a dose-dependent inhibition of cancer cell proliferation, with a marked reduction in cell viability observed at concentrations above 0.5 mg/mL (Figs. 5 and 6). The calculated IC_{50} values were 0.82 ± 0.07 mg/mL for DLD-1 and 0.87 ± 0.06 mg/mL for CAPAN-1, while L929 exhibited an IC_{50} greater than 1 mg/mL, indicating selective cytotoxicity toward cancer cells. At 1 mg/mL, CAPAN-1 and DLD-1 cells displayed viability reductions of over 70%, whereas L929 cells were significantly less affected, highlighting the selective cytotoxicity of the extract, a property of high therapeutic importance for anticancer drug development. It should be noted that while 1 mg/mL is considered a relatively high concentration for crude plant extracts, this initial screening successfully demonstrated that the extract possesses selective cytotoxic effects, warranting further investigation through bioassay-guided fractionation to isolate and identify the active principles, which may exhibit enhanced potency at lower concentrations. The phytochemical profile of *O. angustissima*, determined through LC–ESI–MS/

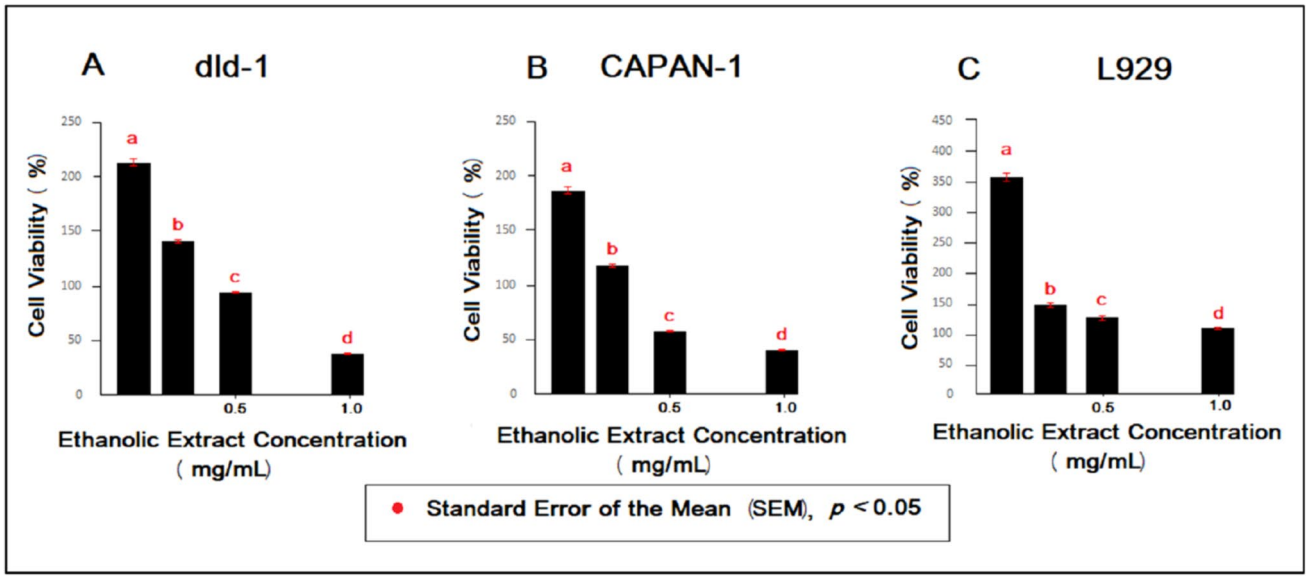


Fig. 5 Cytotoxicity of *Ononis angustissima* ethanolic extract against DLD-1, CAPAN-1, and L929 cell lines. (**A**)-(**C**) indicate statistically significant differences between groups (p 0.05), according to one-way ANOVA followed by Tukey's HSD test

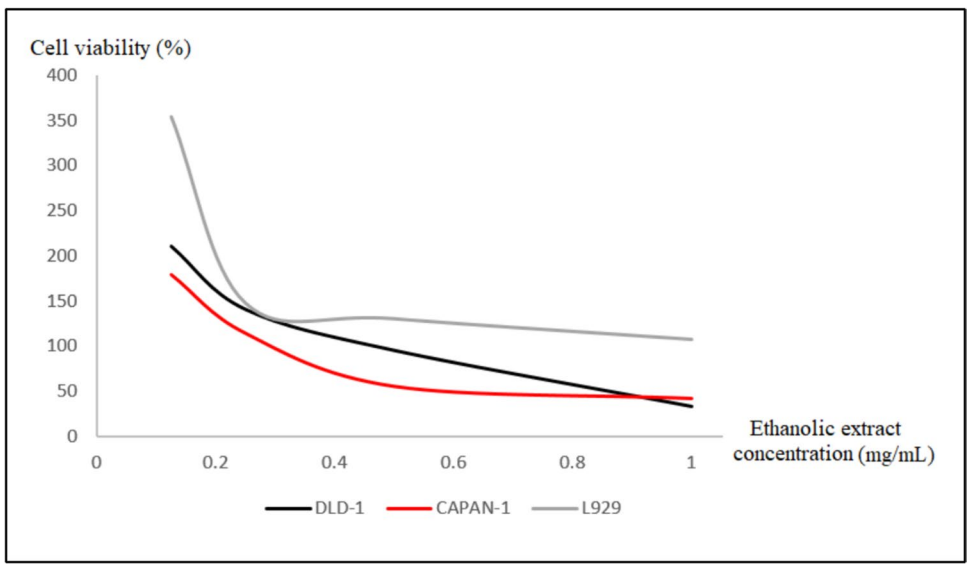


Fig. 6 Dose–response curves of *Ononis angustissima* ethanolic extract against DLD-1, CAPAN-1, and L929 cell lines

MS analysis, provides a plausible explanation for these bioactivities. Luteolin (143.55 ± 1.76 µg/g dw), the most abundant flavonoid, alongside quercetin, baicalein, and isoquercitrin, is known for its pro-apoptotic, anti-inflammatory, and antioxidant mechanisms, which contribute to the suppression of tumor growth and progression (Lin et al. 2008; Luiz-Ferreira et al. 2023; Shahbaz et al. 2023; Cai et al. 2024). Additionally, the high content of salicylic acid (45.82 ± 0.24 µg/gdw) in the extract suggests a complementary mechanism of action, as salicylic acid has been reported to inhibit cyclooxygenase (COX)-mediated inflammatory pathways and induce apoptosis in cancer cells, thereby enhancing the anticancer potential of the extract (Liu et al. 2017; Guenzle et al. 2019).

The findings of our investigation align with and expand on earlier research on the *Ononis* genus. Stojković et al. (2020) investigated the cytotoxic profile of *O. spinosa* methanolic extract and observed no cytotoxic effects on normal human gingival fibroblast (HGF-1) cells at concentrations up to 400 µg/mL, indicating strong biocompatibility. This contrasts with the current results, where *O. angustissima* ethanol extract exhibited significant activity

Table 6 Computational docking scores of selected phytochemicals from *Ononis angustissima* with AChE and BChE enzymes (in silico predictions)

Compound	Binding affinity (kcal/mol)	
	AChE	BChE (1P0I)
Quercetin	− 8.3	− 8.3
Baicalein	− 7.8	− 8.3
Luteolin	− 8.3	− 8.5
Galantamine	− 7.0	− 8.0

AChE acetylcholinesterase, *BChE* butyrylcholinesterase

against cancer cells while maintaining a relatively mild effect on L929 fibroblasts, thereby combining efficacy with selectivity. Similarly, Youssef et al. (2024) reported that ethanol extracts of *O. natrix* showed strong antiproliferative activity against a panel of cancer cell lines, with IC_{50} values of 109 ± 2 µg/mL for CaCo-2 (colorectal adenocarcinoma), 55 ± 2 µg/mL for PC-3 (prostate carcinoma), 68 ± 2 µg/mL for HepG-2 (hepatocellular carcinoma), 123 ± 2 µg/mL for MCF-7 (breast cancer), and 79 ± 1 µg/mL for HeLa (cervical carcinoma). Importantly, their extract demonstrated low cytotoxicity towards normal WI-38 fibroblasts (IC_{50} of 122 ± 4 µg/mL), reinforcing the notion that *Ononis* species hold therapeutic promise as selective anticancer agents with reduced side effects compared to conventional chemotherapeutics.

The significant antiproliferative response observed in CAPAN-1 and DLD-1 cells suggests that *O. angustissima* ethanol extract could act through mechanisms linked to oxidative stress modulation, inhibition of inflammatory mediators, or interference with key signaling pathways such as PI3K/Akt and MAPK (Merecz-Sadowska et al. 2020; Zughaibi et al. 2021). Lu et al. (2017) stated in their study that luteolin was shown to inhibit the phosphorylation of AKT, PI3K, and mTOR within the PI3K signaling cascade, thereby suppressing cell proliferation, inducing cell cycle arrest, and promoting DNA damage and apoptotic progression in colorectal cancer cells through modulation of the MAPK pathway. Such mechanisms are consistent with the known bioactivities of the major flavonoids quantified in *O. angustissima* ethanolic extract, particularly luteolin and quercetin (Almatroodi et al. 2021; Singh and Shukla 2024). These results underscore the high biomedical relevance of *O. angustissima* and also suggest a synergistic interplay between its flavonoid-rich composition and phenolic content, such as salicylic acid (Almatroodi et al. 2021; Bielecka et al. 2025). The selective cytotoxicity observed against cancer cells, coupled with the plant's known antioxidant and anti-enzymatic properties, points to its potential as a multi-target agent for both cancer prevention and therapy (Kopustinskiene et al. 2020).

Molecular Docking

The molecular docking results revealed that the selected compounds from *O. angustissima*, namely luteolin, quercetin, and baicalein, exhibited promising binding affinities toward both AChE and BChE, with docking scores ranging from − 7.8 to − 8.5 kcal/mol (Table 6). Among these, luteolin showed the highest affinity for BChE (− 8.5 kcal/mol), while the reference compound galantamine exhibited a docking score of − 8.0 kcal/mol under the same in silico conditions. Both luteolin and quercetin displayed binding energies of − 8.3 kcal/mol for AChE, compared with − 7.0 kcal/mol for galantamine. These docking results indicate potential binding interactions that warrant experimental validation, suggesting that these flavonoids may possess dual inhibitory potential against cholinesterase enzymes. The predicted interactions can be attributed to their structural features, particularly hydroxyl groups and conjugated aromatic systems, which facilitate hydrogen bonding and π–π stacking within the active sites of cholinesterases (Singh et al. 2022). Previous studies have also highlighted luteolin and quercetin as cholinesterase inhibitors with neuroprotective properties (Imran et al. 2019), supporting the current computational findings. Baicalein, while exhibiting slightly lower affinity for AChE (− 7.8 kcal/mol), demonstrated comparable binding to BChE (− 8.3 kcal/mol), suggesting potential as a selective BChE inhibitor, a characteristic that may be relevant in advanced stages of Alzheimer's disease where BChE activity predominates (Chen et al. 2017).

Quercetin exhibited favorable binding interactions with both AChE and BChE (Fig. 7), with docking scores of − 8.3 kcal/mol for each enzyme. In the AChE binding pocket (Fig. 7a, b), quercetin formed conventional hydrogen bonds with GLN527 and HIS381, along with π-related interactions that contributed to its stabilization within the enzyme's aromatic gorge. In BChE (Fig. 7c, d), quercetin established hydrogen bonds with TYR440, ALA328, and TRP82, as well as stabilizing contacts with GLY116 and PRO285, indicating a binding orientation that may facilitate enzyme inhibition (Liao et al. 2022a, b). These findings align with previous docking studies by Liao et al. (2022a, b), who reported a binding energy of − 8.8 kcal/mol for quercetin with AChE, noting multiple hydrogen bonds with Asp74, Glu202, Gly120, and Tyr133, as well as π–π stacking with Trp86, Tyr337, and Phe338. Similarly, Kurt-Celep et al. (2024) reported that compounds such as isoquercitrin interact with conserved AChE residues, including GLY120, GLY121, PHE338, and TRP86 through π–π and π–sigma interactions associated with inhibitory activity.

Baicalein showed binding energies of − 7.8 kcal/mol with AChE and − 8.3 kcal/mol with BChE (Fig. 8). Within the AChE active site (Fig. 8a, b), baicalein was stabilized by π–π T-shaped interactions and π-alkyl contacts involving

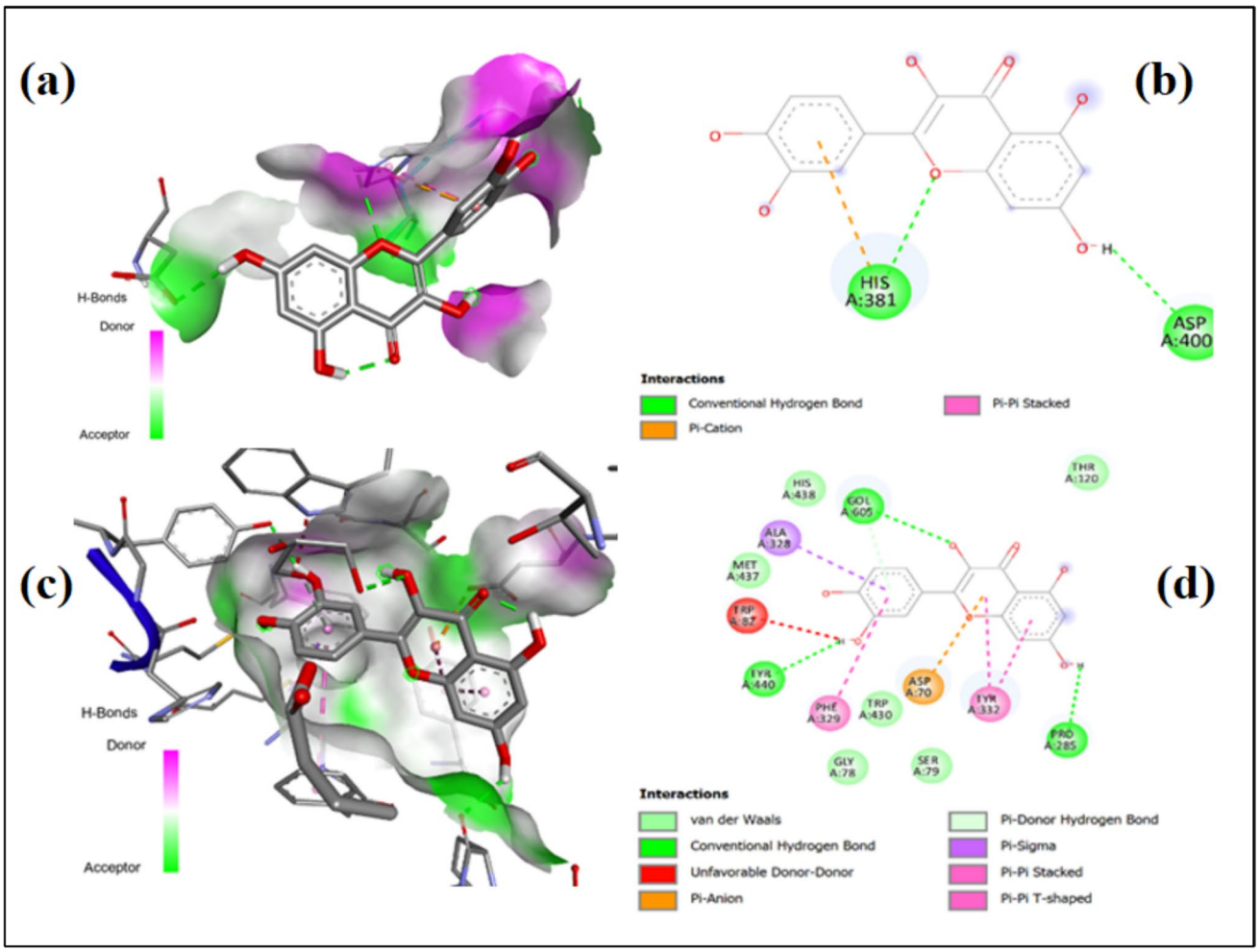


Fig. 7 Active sites of the Alzheimer's disease-related enzymes (AChE and BChE) with quercetin: **a** H-bond interaction between quercetin and AChE; **b** two-dimensional view of the interactions between quercetin and the amino acids of the AChE receptor. **c** H-bond interaction between quercetin and BChE; **d** two-dimensional view of the interactions between quercetin and the amino acids of the BChE receptor

HIS381, TYR382, and ALA528, along with a π–cation interaction. In the BChE binding pocket (Fig. 8c, d), baicalein formed hydrogen bonds with TRP82, ASN83, SER287, GOL605, and THR120, with hydroxyl groups playing a crucial role. This hydrogen-bonding network suggests affinity toward the enzyme, consistent with its predicted inhibitory potential (Chen et al. 2016). These observations are supported by previous in silico studies showing baicalein binding to BACE1 (− 8.6 kcal/mol) through six hydrogen bonds involving its hydroxyl groups (Han et al. 2019), highlighting the recurring role of these moieties in multitarget interactions relevant to Alzheimer's disease therapy (Cacabelos et al. 2024).

The interaction profiles of luteolin, the most abundant metabolite quantified by LC–ESI–MS/MS analysis (Fig. 9), further support its potential as a cholinesterase inhibitor based on computational predictions. Luteolin displayed binding affinities of − 8.3 kcal/mol for AChE and − 8.5 kcal/mol for BChE, which were more favorable than those of galantamine in the docking simulations. In the AChE binding site (Fig. 9a, b), luteolin engaged in hydrogen bonding with GLN527 and HIS381, along with π–π stacking interactions. In BChE (Fig. 9c, d), it formed hydrogen bonds with TYR440, ALA328, and TRP82, and interacted with GLY116 and PRO285. The compound's multiple hydroxyl groups and rigid aromatic structure enable both polar and nonpolar interactions, suggesting potential binding specificity (Juárez-Saldívar et al. 2020). Comparatively, a study on luteolin 7-O-(2″-glucuronyl)-glucuronide, a glycosylated derivative, reported even stronger binding energies of − 10.1 kcal/mol for AChE and − 10.3 kcal/mol for BChE (Stojković et al. 2025), suggesting that glycosylation may enhance binding affinity.

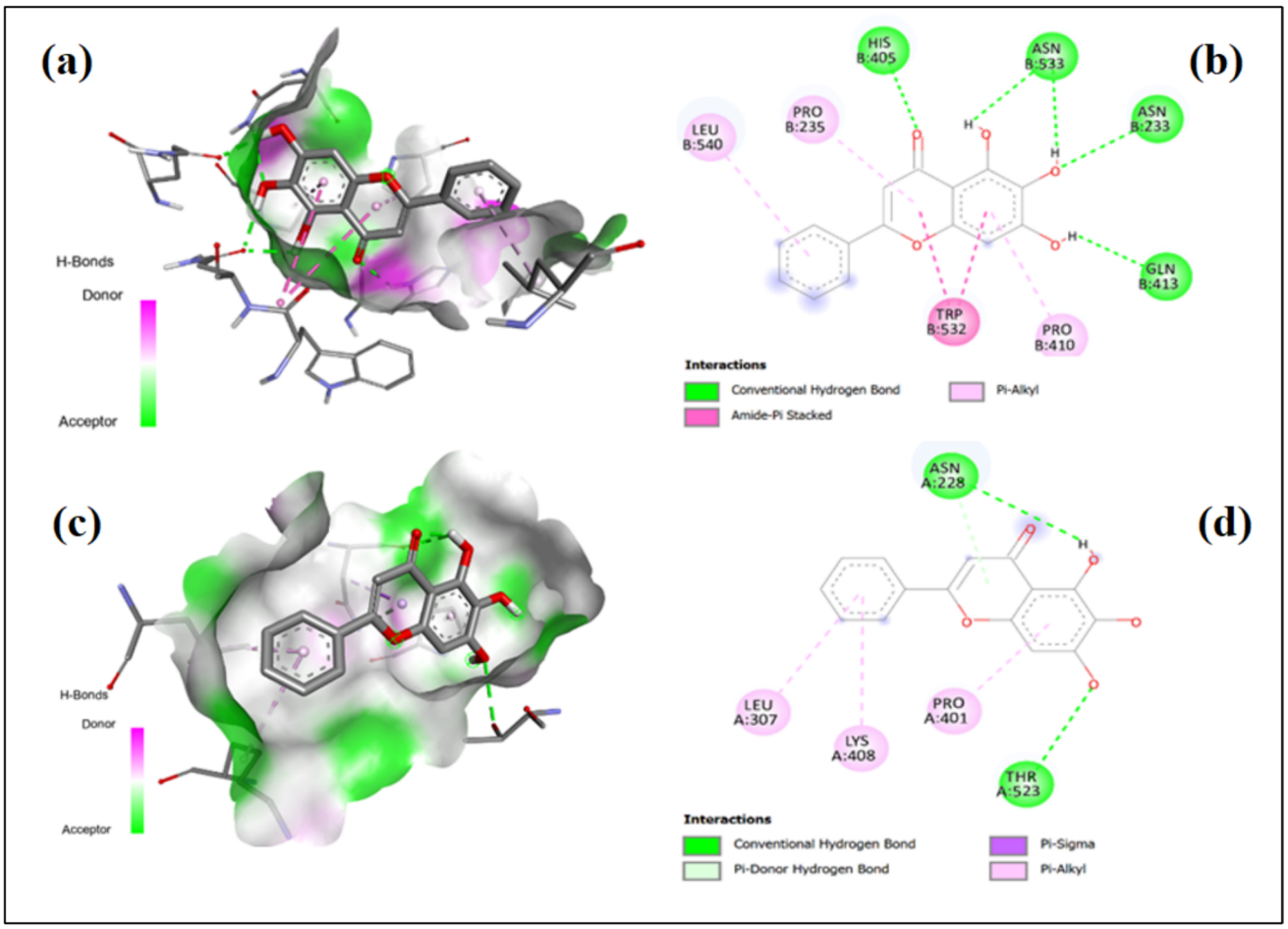


Fig. 8 Active sites of the enzymes Alzheimer's disease (AChE and BChE) with baicalein: **a** H-bond interaction between baicalein and AChE; **b** two-dimensional view of the interactions between baicalein and the amino acids of the AChE receptor. **c** H-bond interaction between baicalein and BChE; **d** two-dimensional view of the interactions between baicalein and the amino acids of the BChE receptor

Galantamine, included as a reference standard, exhibited docking scores of − 7.0 kcal/mol for AChE and − 8.0 kcal/mol for BChE (Fig. 10). In AChE (Fig. 10a, b), galantamine formed π–cation and π–alkyl interactions with HIS381, TYR382, ALA397, and ALA528, with fewer hydrogen bonds than the flavonoids. In the BChE pocket (Fig. 10c, d), it interacted via hydrogen bonding with TRP82, ASN83, THR120, and GOL605 but lacked the extensive bonding network observed with luteolin and baicalein.

It should be noted that these molecular docking results represent computational predictions rather than experimental confirmation. While docking simulations offer valuable insights into potential binding modes, they cannot fully replicate biological complexity, including solvation effects and protein flexibility (Agu et al. 2023). Accordingly, these in silico findings should be interpreted as hypothesis-generating tools that complement but do not replace experimental validation. Future studies employing isolated compounds (particularly luteolin, quercetin, and baicalein) in enzymatic assays are necessary to confirm their true inhibitory potential and binding selectivity.

ADME Analysis

The comprehensive ADME analysis of the 19 bioactive compounds identified in the ethanol extract of *O. angustissima* offers valuable insights into their pharmacokinetic behavior and therapeutic potential. The evaluation of physicochemical properties presented in Table 7 reveals crucial structure–activity relationships that govern their biological effects.

Smaller molecular weight compounds such as gallic acid with molecular weight 154.12, and protocatechuic acid, with molecular weight 290.27, demonstrate favorable absorption characteristics, consistent with Lipinski's Rule of Five (Lipinski et al. 1997; Roumaissa et al. 2025). These compounds exhibit optimal lipophilicity values, with gallic acid showing Log *P* 0.65 and protocatechuic acid Log *P* 0.85,

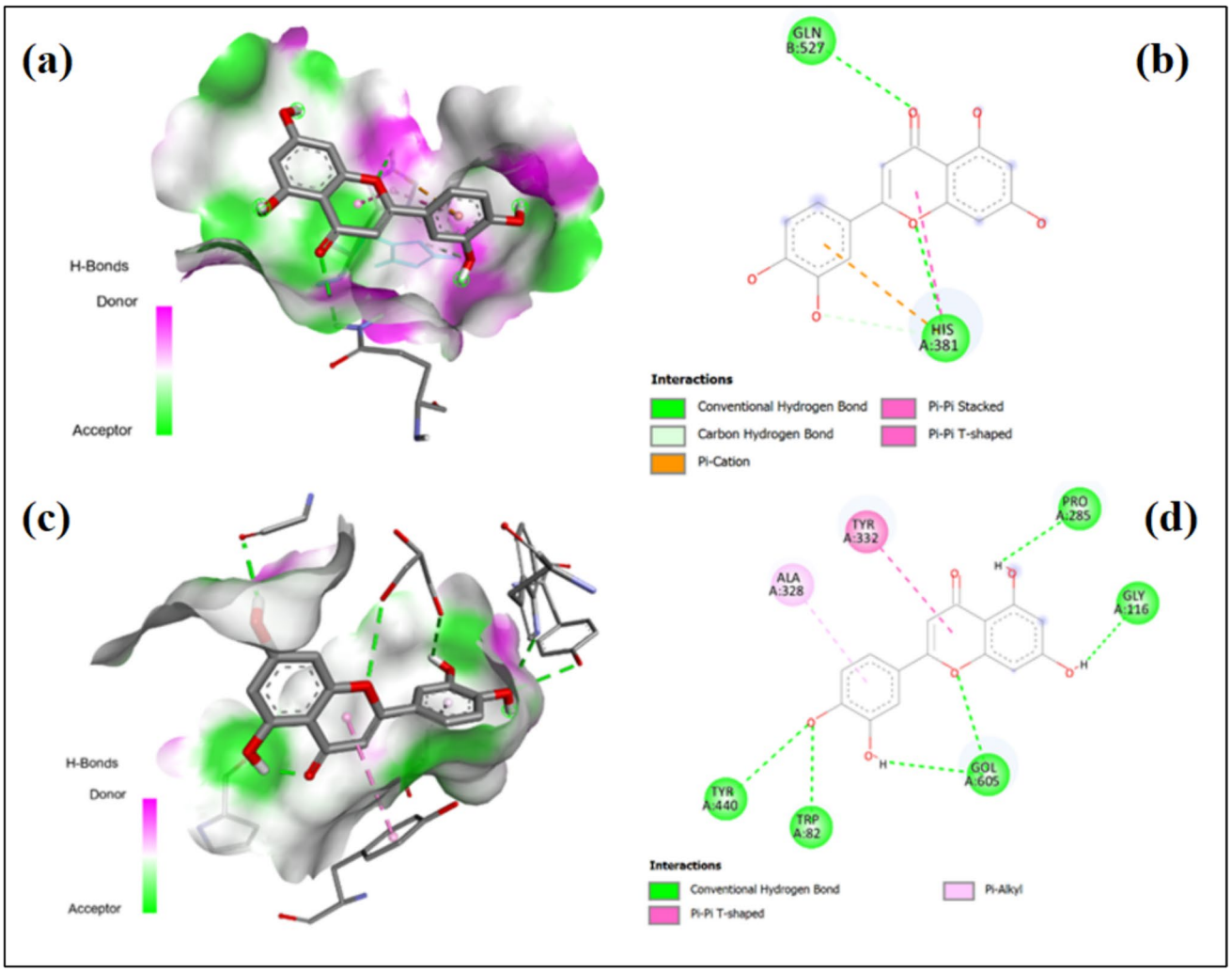


Fig. 9 Active sites of the Alzheimer's disease-related enzymes (AChE and BChE) with luteolin: **a** H-bond interaction between luteolin and AChE; **b** two-dimensional view of the interactions between luteolin and the amino acids of the AChE receptor. **c** H-bond interaction between luteolin and BChE; **d** two-dimensional view of the interactions between luteolin and the amino acids of the BChE receptor

suggesting good membrane permeability. The analysis highlights significant variability in absorption potential among the identified compounds. While phenolic acids like caffeic acid, with Log *P* 1.08, and trans-ferulic acid, with Log *P* 0.62, show high gastrointestinal absorption scores, larger molecules such as chlorogenic acid, with a molecular weight of 354.31 and Log *P* of − 0.38, face substantial bioavailability challenges (Zhang et al. 2022). The topological polar surface area values further support these observations, with compounds like hydroxybenzaldehyde showing a favorable TPSA of 37.3 $Å^2$ compared with kaempferol-3-glucoside with TPSA 210.51 $Å^2$. Blood–brain barrier penetration emerges as a critical differentiator among these compounds. While most exhibit limited CNS access, hydroxybenzaldehyde and o-coumaric acid demonstrate predicted BBB permeability, potentially contributing to the plant's neuroprotective effects. This finding gains particular relevance when considering the cholinesterase inhibitory activity reported for *O. angustissima* extracts. The metabolic stability predictions reveal important considerations, with baicalein and luteolin showing significant CYP450 inhibition potential, including CYP1A2, CYP2D6, and CYP3A4 enzymes (Upadhyay 2014; Chahna et al. 2025). The bioavailability scores range from 0.11 for chlorogenic acid to 0.85 for several phenolic acids, with luteolin presenting particularly promising characteristics. This abundant compound, present at 143.55 ± 1.76 µg/g dw, combines moderate lipophilicity (Log *P* 1.23) with good absorption properties, supporting its potential as a candidate compound for further investigation (Javed et al. 2025). However, it should be noted that these pharmacokinetic parameters were obtained from in silico prediction models and, therefore, represent preliminary estimations of ADME behavior. Experimental studies, such as permeability and metabolic stability assays, would

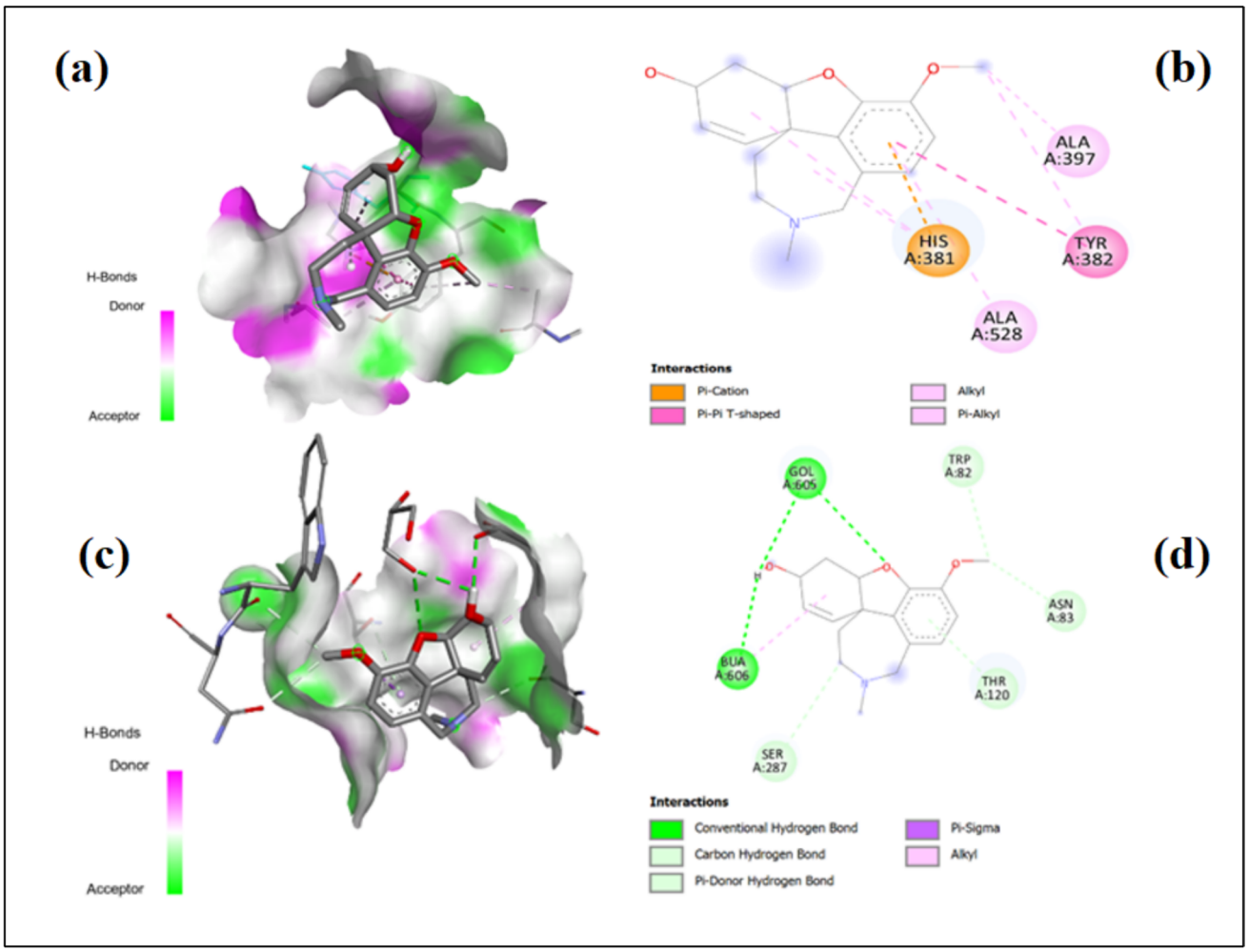


Fig. 10 Active sites of the Alzheimer's disease-related enzymes (AChE and BChE) with galantamine: **a** H-bond interaction between galantamine and AChE; **b** two-dimensional view of the interactions between galantamine and the amino acids of the AChE receptor. **c** H-bond interaction between galantamine and BChE; **d** two-dimensional view of the interactions between galantamine and the amino acids of the BChE receptor

be required to confirm these predictions. The current analysis suggests several important directions for future research. First, the favorable drug-like properties of luteolin, caffeic acid, and trans-ferulic acid warrant prioritized investigation. In addition, formulation strategies should be explored to enhance the bioavailability of promising but poorly absorbed compounds such as chlorogenic acid. Furthermore, the significant CYP450 inhibition potential of several compounds necessitates careful evaluation of potential herb–drug interactions in clinical applications. Overall, these results provide preliminary insights into the possible pharmacokinetic behavior of the identified compounds rather than definitive evidence of pharmacokinetic suitability. Figure 11 displays the molecular distribution of *O. angustissima's* ethanolic extract based on the boiled-egg model. This model evaluates molecule–phase interactions, offering valuable insights into their bioactivity potential and partitioning behavior within the system.

While in silico ADME predictions provide valuable preliminary insights into the pharmacokinetic properties of the identified compounds, certain inherent limitations should be acknowledged. Computational models, despite their utility, cannot fully replicate the complex in vivo physiological environment, including factors such as active transport, metabolic saturation, and inter-individual variability (Lipinski et al. 1997). Consequently, specific predictions warrant particular caution. The observed CYP450 inhibition for compounds such as baicalein, luteolin, and biochanin A suggests potential herb–drug interactions requiring experimental validation (Upadhyay 2014), while compounds with high TPSA values or low predicted gastrointestinal absorption may face bioavailability constraints in vivo despite favorable computational scores (Zhang et al. 2022). These in silico findings

Table 7 The absorption, distribution, metabolism, and excretion (ADME) properties of compounds identified in *Ononis angustissima*

Molecule	1	2	3	4	5	6	7	8	9	10	11	12	13	14	15	16	17	18	19
Physicochemical properties/lipophilicity																			
Molecular weight	154.12	290.27	354.31	122.12	168.15	180.16	152.15	138.12	164.16	390.38	228.24	194.18	464.38	610.52	610.56	448.38	286.24	302.24	286.24
No. rotatable bonds	1	1	5	1	2	2	2	1	2	5	2	3	4	6	7	4	1	1	1
No. H-bond acceptors	4	6	9	2	4	4	3	3	3	8	3	4	12	16	15	11	6	7	6
No. H-bond donors	3	5	6	1	2	3	1	2	2	6	3	2	8	10	8	7	4	5	4
Consensus Log $P_{o/w}$	0.65	0.85	−0.38	1.17	1.08	0.93	1.2	1.24	1.26	0.62	2.48	1.36	−0.25	−1.29	−0.72	−0.25	1.55	1.23	1.58
TPSA ($Å^2$)	77.76	110.38	164.75	37.3	66.76	77.76	46.53	57.53	57.53	139.84	60.69	66.76	210.51	269.43	234.29	190.28	111.13	131.36	111.13
Druglikeness/bioavailability/pharmacokinetics																			
GI absorption	High	High	Low	High	High	High	High	High	High	High	High	High	Low	Low	Low	Low	High	High	High
BBB permeant	No	No	No	Yes	No	No	Yes	Yes	Yes	No	Yes	Yes	No	No	No	No	No	No	No
Log *Kp* (cm/s)	−6.42	−7.82	−8.76	−6.09	−6.31	−6.58	−6.37	−5.54	−6.26	−7.95	−5.47	−6.41	−8.88	−10.26	−10.12	−8.52	−6.65	−7.05	−6.7
Bioavailability score	0.56	0.55	0.11	0.55	0.85	0.56	0.55	0.85	0.85	0.55	0.55	0.85	0.17	0.17	0.17	0.17	0.55	0.55	0.55
Synthetic accessibility	1.07	3.5	4.16	1	1.42	1.81	1.15	1	1.61	4.82	2.02	1.93	5.32	6.52	6.34	5.29	3.16	3.23	3.14
CYP1A2 inhibitor	No	No	No	No	No	No	No	No	No	No	Yes	No	No	No	No	No	Yes	Yes	Yes
CYP2C19 inhibitor	No	No	No	No	No	No	No	No	No	No	No	No	No	No	No	No	No	No	No
CYP2C9 inhibitor	No	No	No	No	No	No	No	No	No	No	Yes	No	No	No	No	No	No	No	No
CYP2D6 inhibitor	No	No	No	No	No	No	No	No	No	No	No	No	No	No	No	No	Yes	Yes	Yes
CYP3A4 inhibitor	Yes	No	No	No	No	No	No	No	No	No	Yes	No	No	No	No	No	Yes	Yes	Yes

BBB blood–brain barrier, *TPSA* topological polar surface area, *GI* gastrointestinal; *Log P*, lipophilicity; *1*, gallic acid; *2*, protocatechuic acid; *3*, chlorogenic acid; *4*, hydroxybenzaldehyde; *5*, caffeic acid; *6*, vanillin; *7*, o-coumaric acid; *8*, salicylic acid; *9*, taxifolin; *10*, trans-ferulic acid; *11*, hesperidin; *12*, isoquercitrin; *13*, kaempferol-3-glucoside; *14*, chrysin; *15*, trans-cinnamic acid; *16*, quercetin; *17*, baicalein; *18*, luteolin; *19*, biochanin A

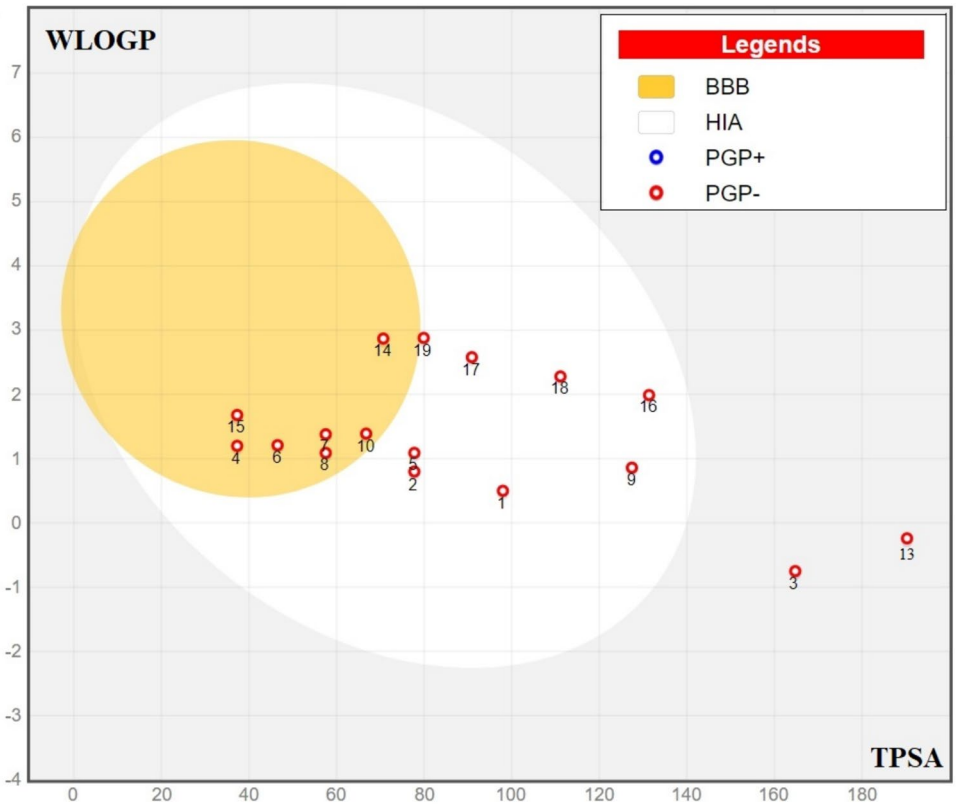


Fig. 11 The boiled-egg model depicts the gastrointestinal absorption and blood–brain barrier permeability of compounds detected and quantified by LC–ESI–MS/MS analysis in the ethanol extract of *O. angustissima*. 1, gallic acid; 2, protocatechuic acid; 3, chlorogenic acid; 4, hydroxybenzaldehyde; 5, caffeic acid; 6, vanillin; 7, o-coumaric acid; 8, salicylic acid; 9, taxifolin; 10, trans-ferulic acid; 11, hesperidin; 12, isoquercitrin; 13, kaempferol-3-glucoside; 14, chrysin; 15, trans-cinnamic acid; 16, quercetin; 17, baicalein; 18, luteolin; 19, biochanin A

should therefore be interpreted as hypothesis-generating tools rather than definitive evidence, necessitating confirmation through experimental approaches such as permeability assays, metabolic stability studies, and in vivo pharmacokinetic evaluations.

Conclusion

This study offers valuable insight into the chemical composition and therapeutic potential of *Ononis angustissima*, a limitedly studied endemic plant in Algeria that is largely used in folk medicine, through a multidisciplinary evaluation of its phytochemical composition, enzyme inhibitory properties, cytotoxic effects, and molecular interactions. The optimized extraction process significantly improved the yield of phenolic and flavonoid compounds, laying the foundation for subsequent bioactivity assessments. LC–ESI–MS/MS profiling identified a range of biologically active constituents, including luteolin, salicylic acid, and trans-ferulic acid—compounds previously associated with anti-enzymatic properties and anticancer activities. The chloroform extract demonstrated selective and potent in vitro anticholinesterase activity, with IC_{50} values surpassing standard inhibitor galantamine, and suggested potential in the management of neurodegenerative disorders such as Alzheimer's disease. Additionally, the ethanol extract showed a strong antiproliferative effect against DLD-1 and CAPAN-1, with limited toxicity toward L929. These cytotoxic responses may stem from the bioactive metabolites in the extract's influence on cell signaling pathways relevant to cancer progression. In silico molecular docking further corroborated these findings, revealing favorable binding affinities and stable interactions between major flavonoids and key residues in the AChE and BChE active sites. Complementary ADME analysis indicated that key compounds, particularly luteolin, caffeic acid, and trans-ferulic acid, possess favorable absorption, lipophilicity, and bioavailability, while also revealing potential CYP450 inhibition that warrants further evaluation for herb–drug interaction risks. These findings suggest that *O. angustissima* represents a promising botanical source of bioactive compounds with notable anticholinesterase and antiproliferative activities in vitro. The present study provides a foundational basis for future investigations, including bioassay-guided isolation of active constituents, elucidation of molecular mechanisms, and in vivo validation, which are necessary steps to assess its potential relevance for phytopharmaceutical applications targeting cancer and neurodegenerative diseases. As the first investigation of this species, the results contribute to the growing body of knowledge on underutilized medicinal plants and open new perspectives for further research.

Author Contribution Conceptualization, **Ibrahim Demirtas;** methodology, **Larbi Derbak and Radia Ayad**; software, **Radia Ayad**; validation, **Hamdi Bendif**; formal analysis, **Abdesselem Si Mohammed and Mohamed Lamine Rabhi;** investigation, **Larbi Derbak**; resources, **Abdesselem Si Mohammed and Khellaf Rebbas;** data curation, **Abdesselem Si Mohammed and Khellaf Rebbas;** writing—original draft preparation, **Larbi Derbak and Mohamed Lamine Rabhi**; writing—review and editing, **Anis Ahmad Chaudhary, Walid Elfalleh** and **Stefania Garzoli**; visualization, **Ibrahim Demirtas** and **Hamdi Bendif**; supervision, **Stefania Garzoli** and **Hamdi Bendif**; project administration, **Anis Ahmad Chaudhary** and **Hamdi Bendif**; funding acquisition, **Walid Elfalleh** and **Hamdi Bendif**. All authors have read and agreed to the published version of the manuscript.

Funding Open access funding provided by Università degli Studi di Roma La Sapienza within the CRUI-CARE Agreement.

Data Availability The data will be available to the authors upon request.

Declarations

Competing interests The authors declare no competing interests.

Open Access This article is licensed under a Creative Commons Attribution 4.0 International License, which permits use, sharing, adaptation, distribution and reproduction in any medium or format, as long as you give appropriate credit to the original author(s) and the source, provide a link to the Creative Commons licence, and indicate if changes were made. The images or other third party material in this article are included in the article's Creative Commons licence, unless indicated otherwise in a credit line to the material. If material is not included in the article's Creative Commons licence and your intended use is not permitted by statutory regulation or exceeds the permitted use, you will need to obtain permission directly from the copyright holder. To view a copy of this licence, visit http://creativecommons.org/licenses/by/4.0/.

References

Agu PC, Afiukwa CA, Orji OU, Ezeh EM, Ofoke IH, Ogbu CO, Aja PM (2023) Molecular docking as a tool for the discovery of molecular targets of nutraceuticals in diseases management. Sci Rep 13(1):13398

Al-Aboudi A, Afifi FU (2011) Plants used for the treatment of diabetes in Jordan: a review of scientific evidence. Pharm Biol 49(3):221–239

Al-Khalil S, Masalmeh A, Abdalla S, Tosa H, Iinuma M (1995) N-Arachidylanthranilic acid, a new derivative from Ononis natrix. J Nat Prod 58(5):760–763. https://doi.org/10.1021/np50119a018

Almatroodi SA, Alsahli MA, Almatroudi A, Verma AK, Aloliqi A, Allemailem KS, Khan AA, Rahmani AH (2021) Potential therapeutic targets of quercetin, a plant flavonol, and its role in the therapy of various types of cancer through the modulation of various cell signaling pathways. Molecules 26(5):1315. https://doi.org/10.3390/molecules26051315

Alshabi AM, Alkahtani SA, Shaikh IA, Orabi MAA, Abdel-Wahab BA, Walbi IA, Habeeb MS, Khateeb MM, Shettar AK, Hoskeri JH (2022) Tribulus terrestris cytotoxicity against breast cancer MCF-7 and lung cancer A549 cell lines is mediated via activation of apoptosis, caspase-3, DNA degradation, and suppressing Bcl-2 activity. Separations 9(11):383. https://doi.org/10.3390/separations9110383

Altuner EM, Ceter T, Işlek C (2010) Investigation of antifungal activity of Ononis spinosa L. ash used for the therapy of skin infections as folk remedies. Mikrobiyol Bul 44(4):633–639

Ameur S, Toumi M, Bendif H, Derbak L, Yildiz I, Rebbas K, Demirtas I, Flamini G, Bruno M, Garzoli S (2024) Cistus libanotis from Algeria: phytochemical analysis by GC/MS, HS-SPME-GC/MS, LC–MS/MS and its anticancer activity. J Food Compos Anal 136:106747

Ausina P, Branco JR, Demaria TM, Esteves AM, Leandro JGB, Ochioni AC, Mendonça APM, Palhano FL, Oliveira MF, Abou-Kheir W, Sola-Penna M, Zancan P (2020) Acetylsalicylic acid and salicylic acid present anticancer properties against melanoma by promoting nitric oxide-dependent endoplasmic reticulum stress and apoptosis. Sci Rep. https://doi.org/10.1038/s41598-020-76824-6

Azeem M, Haider MZ, Javed S, Saleem MH, Alatawi A (2022) Drought stress amelioration in maize (Zea mays L.) by inoculation of Bacillus spp. strains under sterile soil conditions. Agriculture 12(1):50. https://doi.org/10.3390/agriculture12010050

Benmeddour T, Messaoudi K, Flamini G (2024) First investigation of the chemical composition, antioxidant, antimicrobial and larvicidal activities of the essential oil of the subspecies Ononis angustissima Lam. subsp. filifolia Murb. Nat Prod Res. https://doi.org/10.1080/14786419.2024.2305211

Benouchenne D, Bellil I, Akkal S, Bensouici C, Khelifi D (2020) LC–MS/MS analysis, antioxidant and antibacterial activities of Algerian fir (*Abies numidica* de LANNOY ex CARRIÈRE) ethyl acetate fraction extracted from needles. J King Saud Univ Sci 32:3321–3327

Besbas, S. (2020). Secondary metabolites of Ononis mitissima L. (Fabaceae) and biological evaluation (Doctoral dissertation, University of Hadj Lakhdar – Batna 1, Faculty of Material Sciences, Department of Chemistry, Batna, Algeria)

Bhuia MS, Chowdhury R, Akter MA, Ali MA, Afroz M, Akbor MS, ... Islam MT (2024) A mechanistic insight into the anticancer potentials of resveratrol: Current perspectives. Phytother Res 38(8):3877–3898. https://doi.org/10.1002/ptr.8239

Bielecka I, Natorska-Chomicka D, Dołomisiewicz W, Fortes AR, Szewczyk KDS (2025) Phytochemical profile and selective anticancer activity of *Parietaria judaica* L. extracts. Molecules 30(13):2739. https://doi.org/10.3390/molecules30132739

Boncler M, Różalski M, Krajewska U, Podsędek A, Watala C (2013) Comparison of PrestoBlue and MTT assays of cellular viability in the assessment of anti-proliferative effects of plant extracts on human endothelial cells. J Pharmacol Toxicol Methods 69(1):9–16. https://doi.org/10.1016/j.vascn.2013.09.003

Bouheroum M, Zaiter L, Benayache S, Benayache F, Bermejo JB, Leon F, Garcia V (2009) Four flavonoids from the aerial part of Ononis angustissima species. Chem Nat Compd 45(6):874–875. https://doi.org/10.1007/s10600-010-9482-z

Cacabelos R, Martínez-Iglesias O, Cacabelos N, Carrera I, Corzo L, Naidoo V (2024) Therapeutic options in Alzheimer's disease: from classic acetylcholinesterase inhibitors to multi-target drugs with pleiotropic activity. Life (Basel) 14(12):1555. https://doi.org/10.3390/life14121555

Cai J, Tan X, Hu Q, Pan H, Zhao M, Guo C, Zeng J, Ma X, Zhao Y (2024) Flavonoids and gastric cancer therapy: from signaling pathway to therapeutic significance. Drug Des Devel Ther 18:3233–3253. https://doi.org/10.2147/dddt.s466470

Chahna R, Bendif H, Bouzana A, Derbak L, Haouame I, Çam D, Öztürk M, Rebbas K, Ali MAM, Bensouıci C, Boufahja F, Garzoli S (2025) Salvia lanigera Poiret extracts: study of the phytochemical profiling via GC–MS and HPLC–DAD and bioactivity with ADME analysis. Food Anal Methods. https://doi.org/10.1007/s12161-025-02863-2

Chen D, Oezguen N, Urvil P, Ferguson C, Dann SM, Savidge TC (2016) Regulation of protein-ligand binding affinity by hydrogen bond pairing. Science Advances. https://doi.org/10.1126/sciadv.1501240

Chen Y, Lin H, Yang H, Tan R, Bian Y, Fu T, Li W, Wu L, Pei Y, Sun H (2017) Discovery of new acetylcholinesterase and butyrylcholinesterase inhibitors through structure-based virtual screening. RSC Adv 7(6):3429–3438

Chen ZR, Huang JB, Yang SL, Hong FF (2022) Role of cholinergic signaling in Alzheimer's disease. Molecules (Basel) 27(6):1816

Derbak L, Bendif H, Ayad R, Bensouici C, Yildiz İ, Demirtas I, Rebbas K, Plavan G, Ben Hamadi N, Abu-Elsaoud AM, Alomran MM, Özdemir S, Boufahja F (2024) Optimization of polyphenol extraction, phenolic profile by LC-ESI-MS/MS, antioxidant, anti-enzymatic, and cytotoxic activities of Physalis acutifolia. Open Chem 22(1):20240040

Derbak L, Bendif H, Ayad R, Rebbas K, Demirtas I, Yildiz I, Boufahja F, Garzoli S (2025) Extraction process and phenolic profiling of Glebionis coronaria: insight into antioxidant and cytotoxic activities with ADME-based therapeutic potential. Food Anal Methods. https://doi.org/10.1007/s12161-025-02818-7

El Sayed AM, Basam SM, El-Naggar EMBA, Marzouk HS, ElHawary S (2020) LC MS/MS and GC–MS profiling as well as the antimicrobial effect of leaves of selected Yucca species introduced to Egypt. Sci Rep 10(1):17778

Ellman GL, Courtney KD, Andres V Jr., Featherstone RM (1961) A new and rapid colorimetric determination of acetylcholinesterase activity. Biochem Pharmacol 7:88–90

Eswaran SP, Balasubramaniam S, Sakthivel A, Sampath M, Sivanandhan G, Gnanajothi K (2025) Unlocking medicinal benefits and augmenting secondary metabolite synthesis in cultivated and wild legumes. In: CRC Press eBooks (pp. 355–365). https://doi.org/10.1201/9781003475491-26

Fang L, Pan Y, Muzyka JL, Zhan C (2011) Active site gating and substrate specificity of butyrylcholinesterase and acetylcholinesterase: insights from molecular dynamics simulations. J Phys Chem B 115(27):8797–8805. https://doi.org/10.1021/jp112030p

Ganai SA, Sheikh FA, Baba ZA, Mir MA, Mantoo MA, Yatoo MA (2021) Anticancer activity of the plant flavonoid luteolin against preclinical models of various cancers and insights on different signalling mechanisms modulated. Phytother Res 35(7):3509–3532. https://doi.org/10.1002/ptr.7044

Ghribi L, Waffo-Téguo P, Cluzet S, Marchal A, Marques J, Mérillon J, Jannet HB (2015) Isolation and structure elucidation of bioactive compounds from the roots of the Tunisian Ononis angustissima L. Bioorganic & Medicinal Chemistry Letters 25(18):3825–3830. https://doi.org/10.1016/j.bmcl.2015.07.076

Gidaro MC, Alcaro F, Carradori S, Costa G, Vullo D, Supuran CT, Alcaro S (2015) Eriocitrin and apigenin as new carbonic anhydrase VA inhibitors, from a virtual screening of Calabrian natural products. Planta Med 81:533–540

Gökhan Z, Guler GO, Aktumsek A, Ceylan R, Picot CMN, Mahomoodally MF (2015) Enzyme inhibitory properties, antioxidant activities, and phytochemical profile of three medicinal plants from Turkey. Adv Pharmacol Sci 2015:410675. https://doi.org/10.1155/2015/410675

Guenzle J, Garrelfs NWC, Goeldner JM, Weyerbrock A (2019) Cyclooxygenase (COX) inhibition by acetyl salicylic acid (ASA) enhances antitumor effects of nitric oxide in glioblastoma in vitro. Mol Neurobiol 56(9):6046–6055. https://doi.org/10.1007/s12035-019-1513-6

Han J, Ji Y, Youn K, Lim G, Lee J, Kim DH, Jun M (2019) Baicalein as a potential inhibitor against BACE1 and AChE: mechanistic comprehension through in vitro and computational approaches. Nutrients 11(11):2694. https://doi.org/10.3390/nu11112694

He M, Yin Y, Yu G, Zhou H (2024) Phytoestrogens: pharmacological potential and therapeutic insights for urinary tract infections. Phytother Res. https://doi.org/10.1002/ptr.8429

Imran M, Rauf A, Abu-Izneid T, Nadeem M, Shariati M, Khan I, Imran A, Orhan I, Rizwan M, Atif M, Gondal T, Mubarak M (2019) Luteolin, a flavonoid, as an anticancer agent: a review. Biomed Pharmacother 112:108612. https://doi.org/10.1016/j.biopha.2019.108612

Javed A, Mahmood T, Ahsan F, Shamim A, Khan A, Srivastava S, Khan I (2026) An in-depth analysis of luteolin regarding its preclinical, clinical and nanoformulations perspectives. Nat Prod J 16(2), e22103155316738. https://doi.org/10.2174/0122103155316738240901181513

Juárez-Saldívar A, Lara-Ramírez EE, Reyes-Espinosa F, Paz-González AD, Villalobos-Rocha JC, Rivera G (2020) Ligand-based and structured-based in silico repurposing approaches to predict inhibitors of SARS-COV-2 MPRO protein. Sci Pharm 88(4):54. https://doi.org/10.3390/scipharm88040054

Karimi N, Valizadeh M (2023) Novel formulations of kaempferol and its monosaccharide derivatives for healing cancers and microbial infections. Micro Nano Bio Aspects 2(3):7–12. https://doi.org/10.22034/mnba.2023.401346.1036

Katalinić M, Rusak G, Barović JD, Šinko G, Jelić D, Antolović R, Kovarik Z (2009) Structural aspects of flavonoids as inhibitors of human butyrylcholinesterase. Eur J Med Chem 45(1):186–192. https://doi.org/10.1016/j.ejmech.2009.09.041

Kopustinskiene DM, Jakstas V, Savickas A, Bernatoniene J (2020) Flavonoids as anticancer agents. Nutrients 12(2):457. https://doi.org/10.3390/nu12020457

Kouteu P, Kemegne AG, Pahane MM, Fanta ASY, Membangmi AK, Tchamaleu DVT, Agbor GA, Mouangue MR (2024) Face-centered central composite design for the optimization of the extraction of phenolic compounds from kernels and shells of Raphia farinifera and evaluation of the antioxidant, antimicrobial, and anti-inflammatory activities. J Food Process Preserv 2024:1–18. https://doi.org/10.1155/2024/8849005

Kurt-Celep I, Nilofar N, Cetiz MV, Zheleva-Dimitrova D, Gevrenova R, Celep E, Sinan KI, Yildiztugay E, Ferrante C, Zengin G (2024) From small-scale studies to an encompassing view: inhibiting inflammation and clinically relevant enzymes with various extracts of Primula vulgaris using in vitro and in silico techniques. Food Front. https://doi.org/10.1002/fft2.473

Li Y, Zhao J, Hölscher C (2017) Therapeutic potential of Baicalein in Alzheimer's disease and Parkinson's disease. CNS Drugs 31:639–652. https://doi.org/10.1007/s40263-017-0451-y

Liao Y, Hu X, Pan J, Zhang G (2022a) Inhibitory mechanism of Baicalein on acetylcholinesterase: inhibitory interaction, conformational change, and computational simulation. Foods 11(2):168. https://doi.org/10.3390/foods11020168

Liao Y, Mai X, Wu X, Hu X, Luo X, Zhang G (2022b) Exploring the inhibition of quercetin on acetylcholinesterase by multispectroscopic and in silico approaches and evaluation of its neuroprotective effects on PC12 cells. Molecules 27(22):7971. https://doi.org/10.3390/molecules27227971

Lin Y, Shi R, Wang X, Shen H (2008) Luteolin, a flavonoid with potential for cancer prevention and therapy. Curr Cancer Drug Targets 8(7):634–646. https://doi.org/10.2174/156800908786241050

Lipinski CA, Lombardo F, Dominy BW, Feeney PJ (1997) Experimental and computational approaches to estimate solubility and permeability in drug discovery and development settings. Adv Drug Deliv Rev 23(1–3):3–25

Liu J, Ren L, Wang H, Li Z (2023) Isoquercitrin induces endoplasmic reticulum stress and immunogenic cell death in gastric cancer cells. Biochem Genet 61(3):1128–1142. https://doi.org/10.1007/s10528-022-10309-1

Liu Y, Wang Y, Hu Y, Ge S, Li K, Wang S, Li L (2017) The apoptotic inducible effects of salicylic acid on hepatoma cell line: relationship with nitric oxide signaling. J Cell Commun Signal 11(3):245–253. https://doi.org/10.1007/s12079-017-0380-z

Lu X, Li Y, Li X, Aisa HA (2017) Luteolin induces apoptosis in vitro through suppressing the MAPK and PI3K signaling pathways in gastric cancer. Oncol Lett 14(2):1993–2000. https://doi.org/10.3892/ol.2017.6380

Luiz-Ferreira A, Pacifico T, Cruz ÁC, Laudisi F, Monteleone G, Stolfi C (2023) TRAIL-sensitizing effects of flavonoids in cancer. Int J Mol Sci 24(23):16596. https://doi.org/10.3390/ijms242316596

Merecz-Sadowska A, Sitarek P, Śliwiński T, Zajdel R (2020) Anti-inflammatory activity of extracts and pure compounds derived from plants via modulation of signaling pathways, especially PI3K/AKT in macrophages. Int J Mol Sci 21(24):9605. https://doi.org/10.3390/ijms21249605

Mezrag A, Malafronte N, Bouheroum M, Travaglino C, Russo D, Milella L, Severino L, De Tommasi N, Braca A, Dal Piaz F (2017) Phytochemical and antioxidant activity studies on Ononis angustissima L. aerial parts: isolation of two new flavonoids. Natural Product Research 31(5):507–514

Mhadhbi N, Dgachi S, Belgacem S, Ahmed AB, Henry N, Loiseau T, ... Naïli H (2023) Design, theoretical study, druggability, pharmacokinetics and properties evolution of a new organobromocadmate compound as prospective anticancer agent. J Mol Struct 1274:134439. https://doi.org/10.1016/j.molstruc.2022.134439

Mhamdi B, Abbassi F, Abdelly C (2015) Chemical composition, antioxidant and antimicrobial activities of the edible medicinal *Ononis natrix* growing wild in Tunisia. Nat Prod Res 29:1157–1160

Mouillet-Richard S, Ghazi A, Laurent-Puig P (2021) The cellular prion protein and the hallmarks of cancer. Cancers 13(19):5032. https://doi.org/10.3390/cancers13195032

Müller L, Gnoyke S, Popken AM, Böhm V (2010) Antioxidant capacity and related parameters of different fruit formulations. LWT 43(6):992–999. https://doi.org/10.1016/j.lwt.2010.02.004

Mungwari CP, King'ondu CK, Sigauke P, Obadele BA (2024) Conventional and modern techniques for bioactive compounds recovery from plants: review. Sci Afr e02509. https://doi.org/10.1016/j.sciaf.2024.e02509

Nissar J, Masoodi FA, Masoodi L, Ahad T, Furhan J (2024) Response surface methodology (RSM)-based statistical modeling and optimization of the ultrasound-assisted extraction of saffron bioactives. Biomass Convers Biorefin 14(13):14963–14976

Olennikov DN, Kashchenko NI, Chirikova NK, Akobirshoeva A, Zilfikarov IN, Vennos C (2017) Isorhamnetin and quercetin derivatives as anti-acetylcholinesterase principles of marigold (*Calendula officinalis*) flowers and preparations. Int J Mol Sci 18(8):1685. https://doi.org/10.3390/ijms18081685

POWO (2025) Ononis angustissima. https://powo.science.kew.org/taxon/urn:lsid:ipni.org:names:510192-1. Accessed 29 Oct 2025

Paniwnyk L, Cai H, Albu S, Mason TJ, Cole R (2009) The enhancement and scale up of the extraction of antioxidants from *Rosmarinus officinalis* using ultrasound. Ultrason Sonochem 16(2):287–292

Rabhi ML, Zouaoui A, Yildiz I, Salmi I, Metidji H (2025) Chemical characterization of the brown seaweed *Cystoseira compressa* collected from the Algerian coast: a promising source for biostimulant metabolites. Nat Prod Res 1–6. https://doi.org/10.1080/14786419.2025.2478301

Revadigar V, Ghalib RM, Murugaiyah V, Embaby MA, Jawad A, Mehdi SH, Hashim R, Sulaiman O (2014) Enzyme inhibitors involved in the treatment of Alzheimer's disease. Drug Des Discov Alzheim Dis 142–198. https://doi.org/10.1016/b978-0-12-803959-5.50003-9

Roumaissa L, Cherif HS, Derbak L, Venskutonis PR, Demirtas I, Mohammed M A, Boufahja F, Bendif H, Garzoli S (2025) New insights into secondary metabolite potential in *Hypericum perforatum*, UPLC-ESI-MS/MS to novel phytochemical discovery with bioactivity assessment. ChemistrySelect 10(40):e03590

Sadeghi M, Seyedebrahimi S, Ghanadian M, Miroliaei M (2024) Identification of cholinesterases inhibitors from flavonoids derivatives for possible treatment of Alzheimer's disease: in silico and in vitro approaches. Curr Res Struct Biol 7:100146. https://doi.org/10.1016/j.crstbi.2024.100146

Shahbaz M, Naeem H, Momal U, Imran M, Alsagaby SA, Abdulmonem WA, Waqar AB, El-Ghorab AH, Ghoneim MM, Abdelgawad MA, Shaker ME, Umar M, Hussain M, Kumar R, Jbawi EA (2023) Anticancer and apoptosis inducing potential of quercetin against a wide range of human malignancies. Int J Food Prop 26(1):2590–2626. https://doi.org/10.1080/10942912.2023.2252619

Singh D, Shukla G (2024) The multifaceted anticancer potential of luteolin: involvement of NF-κB, AMPK/mTOR, PI3K/Akt, MAPK, and Wnt/β-catenin pathways. Inflammopharmacology. https://doi.org/10.1007/s10787-024-01596-8

Singh S, Arthur R, Upadhayay S, Kumar P (2022) Ferulic acid ameliorates neurodegeneration via the Nrf2/ARE signalling pathway: A review. Pharmacol Res - Mod Chin Med 5:100190. https://doi.org/10.1016/j.prmcm.2022.100190

Singh YP, Tej GNVC, Pandey A, Priya K, Pandey P, Shankar G, Nayak PK, Rai G, Chittiboyina AG, Doerksen RJ, Vishwakarma S, Modi G (2020) Design, synthesis and biological evaluation of novel naturally-inspired multifunctional molecules for the management of Alzheimer's disease. Eur J Med Chem 198:112257. https://doi.org/10.1016/j.ejmech.2020.112257

Stojković D, Dias MI, Drakulić D, Barros L, Stevanović M, Ferreira CFR, Soković D (2020) Methanolic extract of the herb Ononis spinosa L. is an antifungal agent with no cytotoxicity to primary human cells. Pharmaceuticals 13(4):78

Stojković D, Đorđevski N, Rajaković M, Filipović B, Božunović J, Bolevich S, Zengin G, Bolevich S, Gašić U, Soković M (2025) Investigation of bioactive compounds extracted from *Verbena officinalis* and their biological effects in the extraction by four butanol/ethanol solvent combinations. Pharmaceuticals 18(7):1012. https://doi.org/10.3390/ph18071012

Sunil C, Xu B (2019) An insight into the health-promoting effects of taxifolin (dihydroquercetin). Phytochemistry 166:112066. https://doi.org/10.1016/j.phytochem.2019.112066

Topçu G, Ay M, Bilici A, Sarıkürkcü C, Öztürk M, Ulubelen A (2006) A new flavone from antioxidant extracts of *Pistacia terebinthus*. Food Chem 103(3):816–822. https://doi.org/10.1016/j.foodchem.2006.09.028

Upadhyay RK (2014) Drug delivery systems, CNS protection, and the blood brain barrier. Biomed Res Int 2014(1):869269

Vaou N, Stavropoulou E, Voidarou C, Tsakris Z, Rozos G, Tsigalou C, Bezirtzoglou E (2022) Interactions between medical plant-derived bioactive compounds: focus on antimicrobial combination effects. Antibiotics 11(8):1014

Vujanovića M, Zengin G, Đurovićac S, Maškovićd P, Cvetanovića A, Radojkovića M (2019) Biological activity of extracts of traditional wild medicinal plants from the Balkan Peninsula. S Afr J Bot 120:213–218

Yilmaz MA (2020) Simultaneous quantitative screening of 53 phytochemicals in 33 species of medicinal and aromatic plants: A detailed, robust and comprehensive LC–MS/MS method validation. Ind Crop Prod 149:112347. https://doi.org/10.1016/j.indcrop.2020.112347

Youssef AMM, Maaty DaM, Al-Saraireh YM (2024) Qualitative chemical compounds analysis and in vitro estimation of antiproliferative, antidiabetic and anti-Alzheimer's disease effects of Ononis natrix (L.) family Fabaceae. Pharmacia 71:1–11. https://doi.org/10.3897/pharmacia.71.e119755

Zhang Q, Lin L, Ye W (2018) Techniques for extraction and isolation of natural products: a comprehensive review. Chin Med. https://doi.org/10.1186/s13020-018-0177-x

Zhang Y, Cai P, Cheng G, Zhang Y (2022) A brief review of phenolic compounds identified from plants: their extraction, analysis, and biological activity. Nat Prod Commun 17(1):1934578X211069721

Zhou Y, Lu X, Yang H, Chen Y, Wang F, Li J, Tang Z, Cheng X, Yang Y, Xu L, Xia Q (2019) Discovery of selective butyrylcholinesterase (BChE) inhibitors through a combination of computational studies and biological evaluations. Molecules 24(23):4217. https://doi.org/10.3390/molecules24234217

Zughaibi TA, Suhail M, Tarique M, Tabrez S (2021) Targeting PI3K/AKT/MTOR pathway by different flavonoids: a cancer chemopreventive approach. Int J Mol Sci 22(22):12455. https://doi.org/10.3390/ijms222212455

Publisher's Note Springer Nature remains neutral with regard to jurisdictional claims in published maps and institutional affiliations.